THE EFFECTS OF ACOUSTIC VIBRATIONS ON AIR IN A RESONANT HORIZONTAL TUBE WITH AND WITHOUT THROUGHFLOW

A THESIS

Presented to

the Faculty of the Graduate Division

by

Jack Marion Spurlock

In Partial Fulfillment

of the Requirements for the Degree

Doctor of Philosophy in the School

of Chemical Engineering

Georgia Institute of Technology

April 1961

7 D
12 R

THE EFFECTS OF ACOUSTIC VIBRATIONS ON AIR IN A RESONANT HORIZONTAL TUBE WITH AND WITHOUT THROUGHFLOW

Approved:

Thesis Advisor

Date Approved by Chairman: April 27, 1961

"In presenting the dissertation as a partial fulfillment of the requirements for an advanced degree from the Georgia Institute of Technology, I agree that the Library of the Institution shall make it available for inspection and circulation in accordance with its regulations governing materials of this type. I agree that permission to copy from, or to publish from, this dissertation may be granted by the professor under whose direction it was written, or, in his absence, by the dean of the Graduate Division when such copying or publication is solely for scholarly purposes and does not involve potential financial gain. It is understood that any copying from, or publication of, this dissertation which involves potential financial gain will not be allowed without written permission.

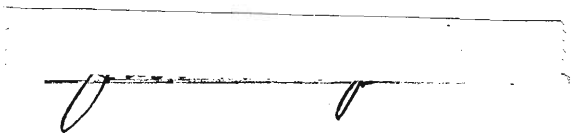

ACKNOWLEDGMENTS

The author is indebted to many individuals who have contributed to the completion of this work. The encouragement, friendship and suggestions of Dr. Henderson C. Ward, who was Thesis Advisor, are sincerely appreciated. The cooperation and advice of Dr. T. W. Jackson and Dr. J. D. Fleming, Jr., who served as members of the thesis committee, are gratefully acknowledged. The research contributions of Mr. K. R. Purdy, Mr. C. C. Oliver and Mr. H. L. Johnson, and the cooperation of Dr. W. F. Atchison and the staff of the Rich Electronic Computer Center were invaluable aids to the author.

The encouragement and spiritual counsel given to the author by his parents through the years provided the inspiration for this work. Further, the patience and understanding provided by the wife and children of the author made this work possible. The gratitude of the author to these people cannot be adequately expressed.

The author would also like to express appreciation to E. I. duPont de Nemours, Inc., for the Summer Research Grants which materially aided the completion of this investigation.

NOMENCLATURE

A_r	Term in the approximation relationship for ber $r(n\omega_f/\nu)^{1/2}$	
A_R	Term in the approximation relationship for ber $R(n\omega_f/\nu)^{1/2}$	
B_r	Term in the approximation relationship for bei $r(n\omega_f/\nu)^{1/2}$	
B_R	Term in the approximation relationship for bei $R(n\omega_f/\nu)^{1/2}$	
C_1	Constant	
C_2	Constant	
C_3	Constant	
C_4	Constant	
$\mathfrak{Q}$	Real-valued imaginary part of a complex expression	
L	Tube length	ft
M_o	Modulus of the complex expression composed of Kelvin's ber and bei functions	
n	Ratio of a resonant frequency to the fundamental resonant frequency (integer)	
p	Modulus of the complex parameter $\beta^2 + i(\omega/\nu)$	ft^{-2}
P	Total pressure at some instant	$lb_m/ft\ sec^2$
$\overline{P}$	Root-mean-square sound pressure	$lb_m/ft\ sec^2$
P_{max}	Maximum pressure in a tube due to acoustic vibrations	$lb_m/ft\ sec^2$

P_{mr}	Reference pressure for a particular sound level meter	$lb_m/ft\ sec^2$
P_r	Reference pressure defined by $P_r = P_{mr}/0.707$	$lb_m/ft\ sec^2$
P_o	Steady-state pressure distribution	$lb_m/ft\ sec^2$
P_1	Amplitude of the transient pressure component	$lb_m/ft\ sec^2$
q	Modulus defined by $q = rp^{1/2}$	
Q	Modulus defined by $Q = Rp^{1/2}$	
r	Radial distance from pipe center and radial coordinate	ft
$\mathfrak{R}$	Real part of complex expression	
Re	Reynolds number	
SPL	Sound pressure level	decibels
t	Time	sec
T_{air}	Air temperature	^oF
U	Total radial velocity component at some instant	ft/sec
U_o	Steady-state velocity component in the radial direction	ft/sec
U_1	Amplitude of the transient velocity component in the radial direction	ft/sec
v	Amplitude of V_1 at a given radius location	ft/sec
V	Total axial velocity component at some instant	ft/sec
V_{mo}	Mean steady-flow velocity in a tube, defined by $V_{mo} = Re\nu/2R$	ft/sec
V_o	Steady-state velocity component in the axial direction	ft/sec
V_1	Amplitude of the transient velocity component in the axial direction	ft/sec

X	Real part of an expression composed of complex terms	
y	Radial distance from tube wall, defined by $y = R - r$	mm
Y	Real-valued imaginary part of an expression composed of complex terms	
z	Axial length and axial coordinate	ft
z_m	Axial distance from tube inlet beyond which effects of β on V_1 are negligible	ft or ins

Greek Letters

α_o	Defined by $\alpha_o = (1/\mu)(\partial P_o/\partial z)$	$(\text{ft sec})^{-1}$
α_1	Defined by $\alpha_1 = n\pi P_r \, e^{SPL/8.68}/L\mu$	$(\text{ft sec})^{-1}$
β	Langhaar's throughflow parameter	ft^{-1}
β_{max}	Maximum negligible value of β	ft^{-1}
Γ	Real part of an expression composed of complex terms	
Δ	Real-valued imaginary part of an expression composed of complex terms	
η	First-quadrant argument, defined by $\eta = \pi - \varphi$	
θ	Angular coordinate	
Θ_o	Argument of the complex expression composed of Kelvin's ber and bei functions	
λ	Wave length of the acoustic vibrations	ft
μ	Dynamic viscosity of a fluid	$\text{lb}_m/\text{ft sec}$
ν	Kinematic viscosity of a fluid	ft^2/sec
ρ	Density of a fluid	lb_m/ft^3
φ	Argument defined by $\varphi = (\Psi + \pi)/2$	

ψ	Argument of the complex parameter $\beta^2 + i(\omega/\nu)$	
ω	Frequency of the acoustic vibrations	rad/sec

Subscripts

b	Condition applicable to the bulk of the tube cross-section
f	Fundamental resonance condition for a given tube length
m	Maximum value beyond which the effects of β on V_1 are negligible
r	Condition at some radial position r
R	Condition at the tube wall where r = R
s	Condition applicable in the domain of the special case where β is negligible
0	Condition at tube centerline where r = 0

TABLE OF CONTENTS

LIST OF TABLES

LIST OF FIGURES

SUMMARY

The combined effects of forced flow and acoustic vibrations on transport phenomena in cylindrical tubes have been of considerable interest in recent years. Although several previous studies have involved the experimental and analytical investigation of the effects of resonant acoustic fields on velocity distributions in fluids inside closed tubes in the absence of throughflow, no treatment of the open-tube system with throughflow has been reported. The investigations reported in the literature which involve open tubes with throughflow have been primarily concerned with the experimental determination of the effects of resonant acoustic vibrations on heat transfer rates and mass transfer rates. However, a principal prerequisite for the analysis of heat and mass transport phenomena is an analytical expression for the velocity distribution in the system.

The purpose of this program of research was the analytical investigation of the effects of acoustic field parameters on the velocity distribution in air inside a resonant, horizontal tube, with and without throughflow. The objectives of this investigation included the adaptation of the equations of motion to include the acoustical parameters, the solution of the resultant mathematical model to yield an expression for the velocity distribution as a function of the system parameters and the analysis of the results obtained from the numerical evaluation of this expression for various flow and acoustical conditions.

The analytical system consisted of a cylindrical tube with a radius R and a length L. A resonant acoustic field of frequency ω and some variable sound pressure level is maintained inside the tube by a loudspeaker mounted at one end of the tube and connected to a sound-generating system. The general system included the forced flow of air through the tube, but a special case involving a system without throughflow was also considered. The system was restricted to the conditions that the air inside the tube has a constant density and viscosity, the forces in the system are symmetrical with respect to the tube axis, the effects due to gravity are negligible, and, for the case involving throughflow, laminar-flow development would take place in the absence of acoustical effects.

It was assumed that the composition of the pressure and each velocity component may be represented as a sum of the steady-state and transient terms. The z-component of the Navier-Stokes equations of motion in cylindrical coordinates for the system subjected to these restrictions was reduced to a linear form by a procedure similar to that employed by Langhaar (Journal of Applied Mechanics, 9, 55 - 58, 1942) in his analytical treatment of laminar-flow development in the entrance length of tubes. This procedure produced a mathematical model for the analytical system in terms of the instantaneous velocity in the axial direction due to acoustical effects V_1. The solution to this model is a complex expression which requires a time-consuming procedure to obtain a numerical evaluation.

The use of complex-variable theory resulted in an analysis of the orders of magnitudes of the terms in the mathematical model. This

analysis yielded a less complicated solution applicable in the domain of the special case when throughflow has no effect on the value of V_1. The results of Langhaar were used to obtain an expression which defines the scope of the domain of this special case. The numerical evaluation of the expression for the scope of the domain of the special case showed that for a tube with a length of four feet and a radius greater than 0.05 ft the less complicated expression for V_1 is applicable over the entire tube length except for a small region at the tube inlet.

The expression for V_1 for the domain of the special case was combined with the continuity equation for the analytical model to yield an expression for the radial component of velocity due to acoustical effects U_1. The analytical expressions for V_1 and U_1 were numerically evaluated at various points (r,z) in the system for selected values of tube radius R (0.058, 0.116 and 0.174 ft), resonant frequency ω (865, 1730, 3460 and 6920 rad/sec) and sound pressure level SPL (140, 145, 150, 155 and 160 db). Corresponding values of U_1 and V_1 at various points in the system were combined to yield an interpretation of the instantaneous velocity effects which take place in the system in the absence of throughflow. The instantaneous directions and magnitudes of the resultant of the radial and axial velocity components due to acoustical effects in the analytical system are greatly influenced by the values of tube radius and the frequency of the acoustic disturbance. Over the range of values included in this investigation, increases in either or both of these parameters resulted in greater influence on the resultant vector by the radial velocity component. These predicted trends are in agreement with the experimental observations of Jackson

and Johnson (AFOSR Technical Report 60-52, 1960) for a closed tube.

The analytical expression for V_1 for the domain of the special case was modified to yield an expression for the absolute value of the velocity profile in the analytical system when the resonance restriction is removed. The numerical evaluation of this expression gave good agreement with experimental data obtained by Meyer and Güth (Acustica, 3, 185 - 187, 1953) for progressive sound waves of approximately the same frequency in the region of a solid boundary.

For the system with throughflow, the instantaneous values of the total velocity component in the axial direction were obtained by the combination of the values of V_1 at various points in the system with corresponding values of the steady-flow velocity component in the axial direction V_o. Values for V_o were calculated by the method of Langhaar at points in the system corresponding to those for which values of V_1 were calculated. Reynolds numbers of 100, 1000 and 2000 were used in the evaluation of V_o. The combination of corresponding values of V_o and V_1 predicted an instantaneous acoustic effect on the normal laminar boundary-layer development which is periodic with respect to axial position in the system. There are no effects at the tube inlet and at velocity nodes, whereas maximum effects occur at velocity loops other than the tube inlet. At higher values of Reynolds number the effects of acoustic vibration on the thickness of the developing boundary layer are significant only at elevated sound pressure levels. The value of sound pressure level below which acoustic effects are negligible decreases with decreases in values of Reynolds number. This analytical effect is in agreement with the results reported by several

investigators who have observed that acoustic vibrations have little or no effect on transport rates when the sound pressure level is decreased below a certain "threshold" value.

Based upon the results of this investigation it is recommended that further analytical development be undertaken to yield an expression for the mean velocity effects due to acoustic vibrations. An expression of this type would be suitable for inclusion in transport rate equations. In addition, flow visualization studies should be conducted to provide more experimental observations of the effects of acoustic vibrations on boundary-layer development.

CHAPTER I

INTRODUCTION

The combined effects of forced flow and acoustic vibrations on transport phenomena in cylindrical tubes have been of considerable interest in recent years. In the area of heat transfer this interest has been intensified by the failure of the tail pipes on jet aircraft and rocket engines which experienced concentrated acoustic effects. Experimentation has indicated that these effects cause an increase in heat transfer rates which may produce failure of the material of which the tail pipes and rocket engines are constructed. Similar intensification of interest has developed in the possibility of utilizing resonant acoustic vibrations to increase mass transfer rates. The important role of mass transfer in transpiration cooling, rocket nose-cone ablation, combustion-zone intermixing and other physical operations of interest in the field of space technology has contributed to this intensification of interest. Mass transfer rate control is also important in the chemical process industries where these rates affect the economy involved in such processes as fuel combustion, catalysis, homogeneous and heterogeneous chemical reactions.

The investigations reported in the literature have been primarily concerned with the experimental determination of the effects of resonant acoustic vibrations on transport rates. The analytical aspects of the combined phenomena have received little treatment. However, a principle prerequisite for the analysis of heat and mass transport phenomena is an

analytical expression for the velocity distribution in the system. A significant need has been created for the development of an analytical expression for the velocity of a fluid in a tube in which a resonant acoustic field has been established. An expression of this type can be incorporated into the respective transport rate equations to yield expressions for the effect of acoustic fields on heat and mass transfer rates, in the system.

Purpose of This Research

The purpose of this program of research was the analytical investigation of the effects of acoustic field parameters on the velocity distribution in air inside a resonant, horizontal tube, with and without throughflow. The objectives of this investigation included the adaptation of the equations of motion to include the acoustical parameters, the solution of the resultant mathematical model to yield an expression for the velocity distribution as a function of the system parameters, and the analysis of the results obtained from the numerical evaluation of this expression for various flow and acoustical conditions.

Related Literature

The technical literature which is of interest in this investigation includes the reports on the results obtained in two related areas of research. One of these areas involves investigations concerned only with the study of resonant acoustic fields. These investigations include experimental and analytical determinations of the resonant fields established inside tubes and around solid objects, and they provide a basic understanding or interpretation of the resonant acoustic phenomena.

The other area involves studies of the effects of acoustic fields on transport rates in fluids by natural and forced convection. The results of the studies in this latter area of research show the importance of continued investigation to determine the mechanism of the resonant acoustical effects.

Resonant acoustic fields.--One of the earliest experimental studies of resonant acoustic fields inside tubes was performed by Kundt. His method of establishing field patterns with dust particles inside tubes by resonating the tubes has been used for many years in physics courses to demonstrate sound fields. An analytical treatise by Lord Rayleigh (1) contains the development of an expression for the velocity distribution which is established in Kundt's tubes and which results in the observed effects. In the same study, Lord Rayleigh considered a system in which the fluid is considered to be compressible and the motion takes place in a two-dimensional system. Simplifications of terms in the applicable Navier-Stokes equations were made and these resulted in a first approximation to the actual mathematical model for the system. The solution to the approximate model in terms of the velocity distribution was adapted for a tube of revolution and yielded the vortical flow pattern shown in Fig. 1. This analysis predicted that particles under the influence of resonant acoustic fields inside tubes would flow in a circulatory manner from the nodes in the sound field to the loops (antinodes) and return to the nodes, obeying continuity and axial symmetry.

A study involving experimental work was conducted by Andrade (2). An acoustically resonant glass tube with a small diameter was filled

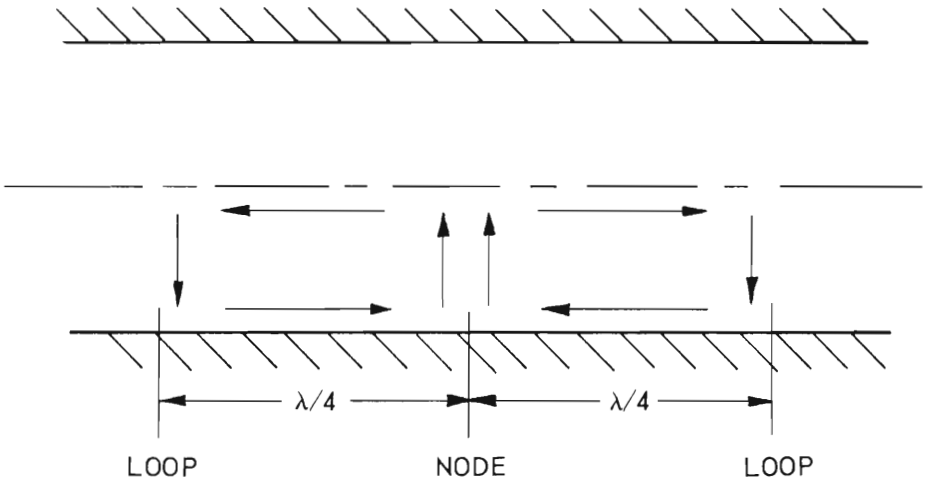

Figure 1. Schematic Representation of the Vortical Flow Cells Predicted by Lord Rayleigh for Particles Inside Resonant Acoustic Tubes.

with smoke and sealed at the end opposite the loud-speaker sound source. Under the influence of the acoustic field the smoke particles flowed in the circulatory manner predicted by Rayleigh. A schematic representation of the flow cells photographed by Andrade is shown in Fig. 2.

In a recent investigation at the Georgia Institute of Technology, Jackson and Johnson (3) studied the various parameters which affect the nature of the flow cells observed by Andrade. Smoke flow patterns similar to those observed by Andrade were produced and photographed in a tube having an inside diameter of 3/4 inch. Samples of the photographic studies of this type of flow pattern for two different frequencies are shown in Fig. 3. The directions of flow and the relative orientation of the cells are the same as those shown schematically in Fig. 2. The investigators were unable to obtain this type of flow in tubes of larger diameter. Flow types for the larger diameter tubes displayed more random turbulent motion and less axial symmetry. Typical results of the photographic studies of the flow in the tubes of larger diameter are shown in Fig. 4. In all these investigations it is apparent that various modes of particle circulation take place and it seems feasible to assume that these circulations could affect transport rates between the circulating medium and the tube wall. Similar circulatory motions are, of course, responsible for the increased thermal rate effects attributed to natural convection heat transfer.

Meyer and Güth (4) reported the results of an elaborate experimental investigation in which they visually studied the acoustic viscous boundary layer for sound waves in air near a rigid surface. Small drops of oil from a sprayer were introduced into the acoustic field inside a tube.

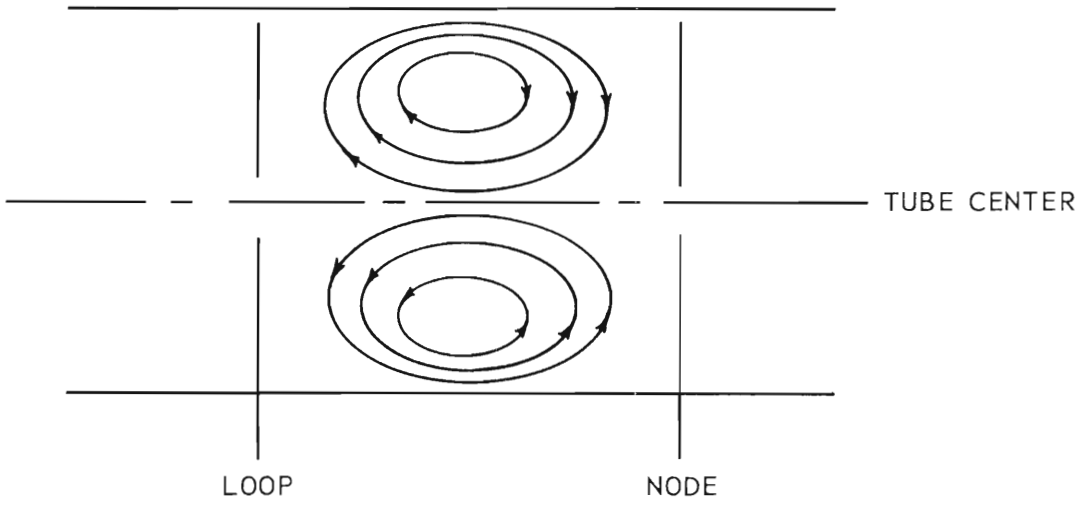

Figure 2. Schematic Representation of the Flow Cells Observed by Andrade in Resonant Tubes.

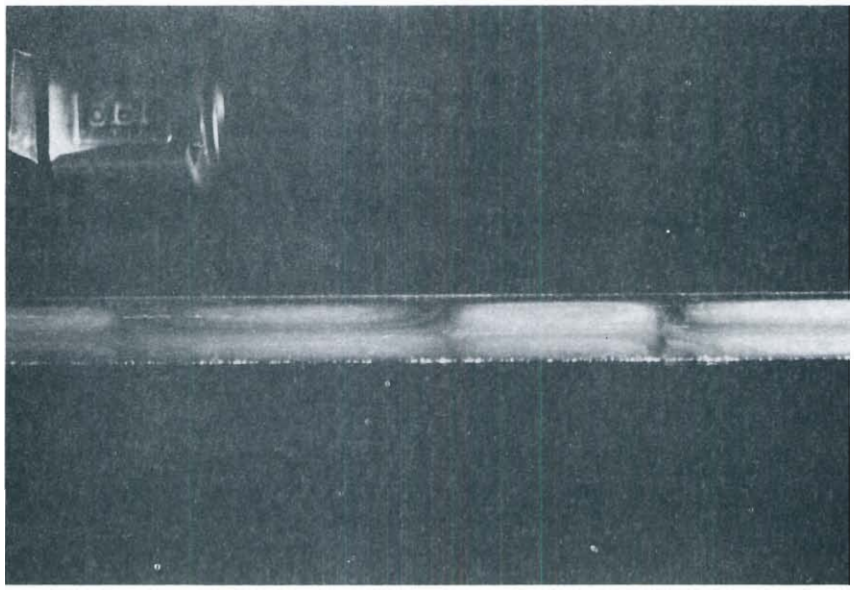

FREQUENCY 1200 CPS

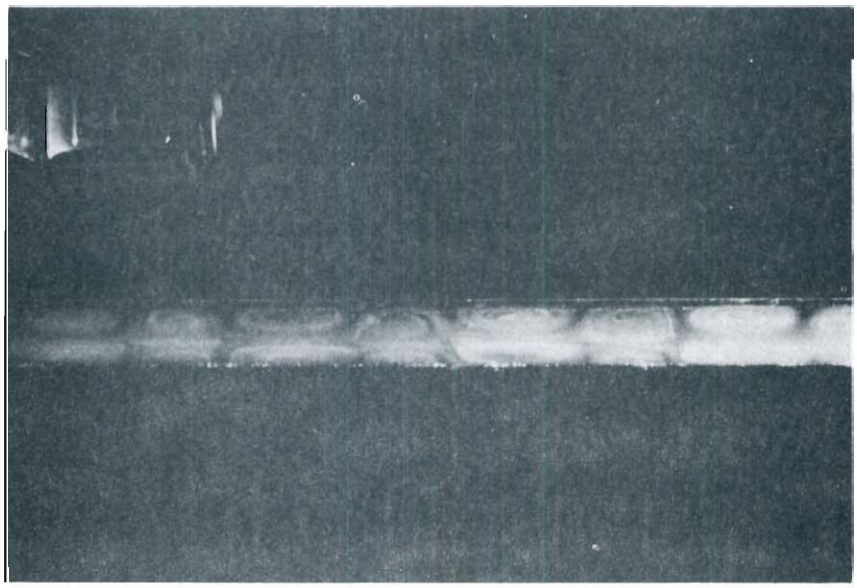

FREQUENCY 2500 CPS

Figure 3. Circulation Cells Produced in a Resonant Horizontal Closed Tube with a Diameter of 3/4 Inch.

a. 5 WATTS
WITH LATEX DIAPHRAGM

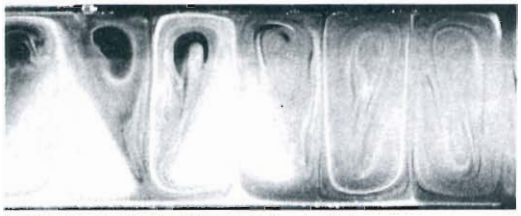

d. 5 WATTS

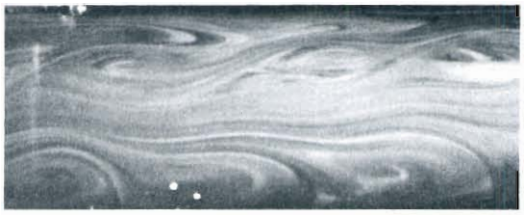

b. 25 WATTS
WITH LATEX DIAPHRAGM

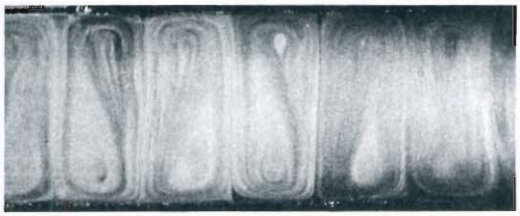

e. 25 WATTS

c. 50 WATTS
WITH LATEX DIAPHRAGM

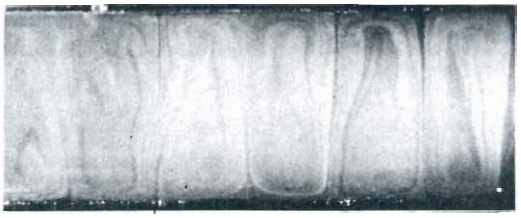

f. 50 WATTS

Figure 4. Flow Patterns Obtained with Smoke in a Resonant Horizontal Closed Tube with a Diameter of 3-11/32 Inches.

The vertical position of the indicator drops was controlled by the action of an external electric field on the charged oil particles. By using an arc light source and a synchronized light beam interrupter, the movement of the oil drops was observed at various vertical distances above a solid boundary. During a typical experiment, results similar to those represented schematically in Fig. 5 were observed. The particle amplitude of vibration was essentially constant beyond the narrow region near the solid surface. As the drops moved nearer the solid surface the influence of the viscous boundary layer produced a reduction in the amplitude of the particle oscillations. The velocity amplitude of the particles in this vicinity diminished gradually at first and then moved rapidly to zero as the particles approached the solid surface. The amplitudes observed in this boundary layer had the form of an exponentially decaying oscillation as a function of distance from the solid surface. The experimental results obtained in this investigation agreed with theoretical deductions reported by Cremer (5).

Other studies have been conducted to investigate the acoustic fields surrounding various bodies. A summary of the results of several investigations of this type is given in a report by Holman and Mott-Smith (6).

Effects of acoustic fields on transport rates.--It is possible to obtain an understanding of some of the general effects produced by superposed sound and heat from the results reported by Kubanskii (7, 8, 9). This investigator studied the effects of acoustic vibrations from eight to thirty kilocycles in frequency on natural-convection heat transfer from a heated horizontal tube immersed in the sound field. In these

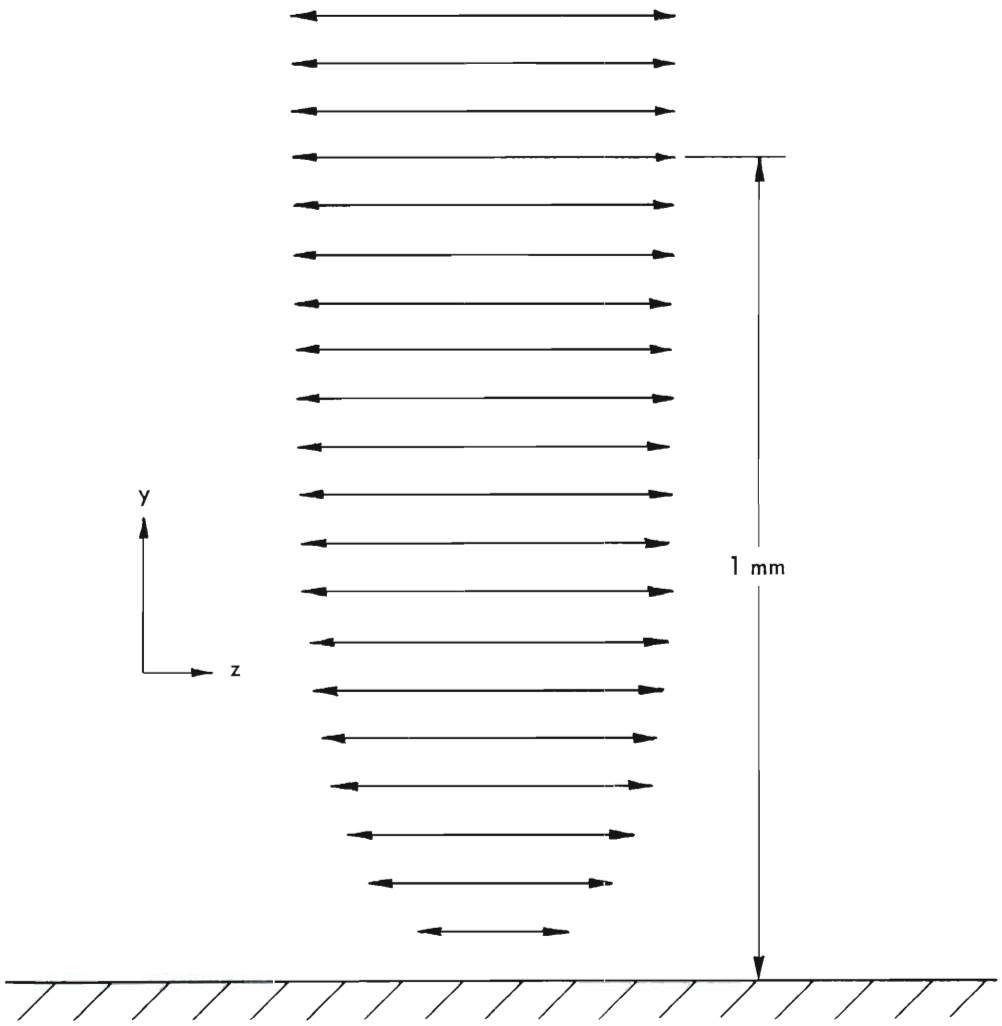

Figure 5. Schematic Representation of the Particle Vibration Amplitudes Observed by Meyer and Güth (4).

experiments, Kubanskii generated a high-intensity sound field around the cylinder with a Hartman vibrator, converting its emissions into a parallel beam with a parabolic reflector. The cylinder was a smooth brass calorimeter tube equipped with an electric heater. Smoke stream studies permitted a qualitative determination of the sound field, and quantitative data were obtained on the actual effects of the sound field on heat transfer from the cylinder. The heat transfer coefficients for natural convection from the heated cylinder were observed to increase by a factor of two or more when standing waves existed around the heated cylinder. The increase was found to be more significant for free convection than for forced convection.

Jackson, Harrison and Boteler (10) performed experiments with a vertical, heated tube through which air was forced at low values of Reynolds number. The system was calibrated without sound to determine the range of the heat transfer coefficients encountered with only free and forced convection heat transfer effects in the tube. Once the system was calibrated, a resonant acoustic field was established in the tube with a speaker driver and horn connected to an audio oscillator and amplifier. Quantitative data included measurements of heat transfer coefficients obtained with free- and forced-convection and acoustic vibration effects, frequencies of the sound field, and sound pressure level values in the plenum chamber at the entrance to the vertical column. The speaker driver and horn were mounted in this entrance plenum chamber. To prevent any distortion in the sound field inside the tube during a data run, no sound pressure level measurements were made during these experiments. It was observed that little or no effect was produced on the heat transfer rates at chamber sound pressure

levels below 118 decibels. Above this threshold value, steady increases in the heat transfer coefficients occurred with increases in sound pressure levels. Similarity and empirical considerations resulted in an expression for the Nusselt number as a function of Reynolds number, Graetz number, sound pressure level and vibration frequency. This expression correlated the experimental data within ±16 per cent.

The results obtained in the investigation just described formed the basis for recent investigations reported by Spurlock, et al., (11) and Jackson, et al., (12). The results reported in both of these references were obtained successively on the same experimental system which consisted of a horizontal double-pipe heat exchanger equipped with chambers for the collection and measurement of condensate. The condensate resulted from the heat transfer between saturated steam in the annular space and air flowing through the inner tube. Compartments in the condensate chamber provided local incremental measurements of the condensate formation rate and permitted the determination of local heat transfer rates and heat transfer coefficients. The system was calibrated without the effects of sound as in the case for the earlier vertical system. After the completion of the calibration tests, the tube was acoustically resonated by a speaker driver mounted at one end of the tube and connected to a sound generating system. Heat transfer rates were determined from measurements recorded at various sound pressure levels, frequencies and air flow rates. These rate values and their respective associated heat transfer coefficient values were compared with the calibration rates and coefficients obtained at corresponding values of Reynolds number. It was observed

that the sound field produced a periodic effect on the local heat transfer coefficients yielding maximum values at velocity nodes. The loop and nodal locations in the tube were determined from resonance theory for open pipes. The maximum observed increase in the local Nusselt number over the no-sound calibration value was 260 per cent at a sound pressure level of 162.5 decibels. At this same sound pressure level a maximum decrease of 71 per cent was obtained. No fundamental analysis was produced in this study but the data were correlated by a semi-empirical expression derived by a technique of superposition of forces.

CHAPTER II

DEVELOPMENT OF THE MATHEMATICAL MODEL

The analytical system for which a mathematical model is derived in this chapter is shown schematically in Fig. 6. The boundary for the system is the inside wall of a cylindrical tube of radius R and length L. A resonant acoustic field of frequency ω and some variable sound pressure level is maintained in the tube by the loudspeaker and its associated sound generating apparatus. Any point of position inside the tube can be described in terms of the cylindrical coordinates r, z, and θ, as shown in Fig. 6. The general system includes the forced flow of air through the tube. A special case involving a system without throughflow was also studied and will be considered later.

The following initial restrictions were imposed upon the analytical system:

a. The density and the viscosity of the air inside the tube are constant.

b. The forces in the system are symmetrical with respect to the z-axis.

c. The effects due to gravity are negligible.

d. The Reynolds numbers based upon the mean velocity of the throughflow of air in the system without any acoustical effects are well within the laminar flow regime.

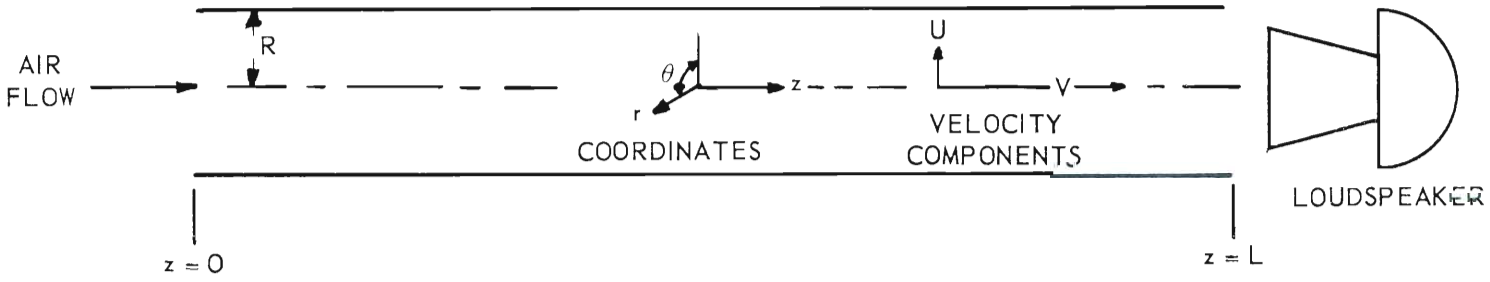

Figure 6. A Schematic Diagram of the Analytical System.

e. $\partial^2 V/\partial z^2$ is negligible such that the derivative of the normal stress is the same as the pressure gradient in the z-direction in an incompressible fluid.

These restrictions are common to model developments for fluid systems and they reduce the z-component of the Navier-Stokes equations of motion in cylindrical coordinates to the form

$$\frac{\partial V}{\partial t} + U \frac{\partial V}{\partial r} + V \frac{\partial V}{\partial z} = - \frac{1}{\rho} \frac{\partial P}{\partial z} + \nu \left[\frac{\partial^2 V}{\partial r^2} + \frac{1}{r} \frac{\partial V}{\partial r} \right] . \tag{1}$$

Since U and V represent the total velocity components in the r- and z-directions, respectively, then both must be composed of steady-state and transient terms. If it is assumed that the composition of the pressure and each velocity component may be represented as a sum of the steady-state and transient terms, expressions for U, V and P can be written in the forms

$$U = U_o + U_1 e^{i\omega t}, \tag{2}$$

$$V = V_o + V_1 e^{i\omega t}, \tag{3}$$

and

$$P = P_o + P_1 e^{i\omega t}. \tag{4}$$

In Equations (2) and (3), U_o and V_o are the steady-state velocity components and are functions of r and z only. Similarly, U_1 and V_1 are the amplitudes of the transient velocity components and they, too, are expressed as function of r and z only. In Equation (4), P_o is the steady-state pressure distribution and is assumed to be a function of

z alone. P_1 is the amplitude of the transient pressure component and is also assumed to be a function of z alone. In Equations (2), (3), and (4), ω is the frequency of the resonant acoustic vibrations which propagate the transient terms in these equations.

A procedure similar to that developed by Langhaar (13) was employed to reduce Equation (1) to a more linear form. The additional restrictions required in this development are:

f. At the tube inlet ($z = 0$), V is a function of time only and at any instant is constant across the inlet cross section.

g. The pressure gradient $-\partial P/\partial z$ is a function of z alone.

h. The term $(U\ \partial V/\partial r) + (V\ \partial V/\partial z)$ may be approximated by the expression $\nu\beta^2 V$, where β is a function of z alone.

Langhaar showed that the approximation made in this last restriction holds, for the case of steady flow, at all points except those in the developing boundary layer. For the case of unsteady flow, irrespective of the value of β, this approximation is satisfied at the tube inlet and at the tube wall. In addition, this approximation provides for any interdependencies among the steady-state and transient terms neglected by Equations (2) and (3).

The substitution of the approximation

$$(U\ \partial V/\partial r) + (V\ \partial V/\partial z) = \nu\beta^2 V$$

into Equation (1) and rearrangement of the resultant expression yields

$$\frac{\partial^2 V}{\partial r^2} + \frac{1}{r}\frac{\partial V}{\partial r} - \beta^2 V = \frac{1}{\mu}\left(\frac{\partial P}{\partial z}\right) + \frac{1}{\nu}\left(\frac{\partial V}{\partial t}\right). \qquad (5)$$

The appropriate partial derivatives of V and P required in Equation (5) are obtained from Equations (3) and (4). These are

$$\frac{\partial V}{\partial r} = \frac{\partial V_o}{\partial r} + \left(\frac{\partial V_1}{\partial r}\right) e^{i\omega t} ,$$

$$\frac{\partial^2 V}{\partial r^2} = \frac{\partial^2 V_o}{\partial r^2} + \left(\frac{\partial^2 V_1}{\partial r^2}\right) e^{i\omega t} ,$$

$$\frac{\partial V}{\partial t} = i\omega V_1 e^{i\omega t} ,$$

and

$$\frac{\partial P}{\partial z} = \frac{\partial P_o}{\partial z} + \left(\frac{\partial P_1}{\partial z}\right) e^{i\omega t} .$$

When these expressions are substituted into Equation (5), the resultant relationship after rearrangement is

$$\left[\frac{\partial^2 V_o}{\partial r^2} + \frac{1}{r}\frac{\partial V_o}{\partial r} - \beta^2 V_o - \frac{1}{\mu}\frac{\partial P_o}{\partial z}\right] = -e^{i\omega t}\left[\frac{\partial^2 V_1}{\partial r^2} + \frac{1}{r}\frac{\partial V_1}{\partial r} - \left(\frac{i\omega}{\nu} + \beta^2\right) V_1 - \frac{1}{\mu}\frac{\partial P_1}{\partial z}\right]. \quad (6)$$

The expression in terms of V_o and P_o on the left side of Equation (6) is identical with the equation of motion for steady flow as expressed by Langhaar in the form

$$\frac{\partial^2 V_o}{\partial r^2} + \frac{1}{r}\frac{\partial V_o}{\partial r} - \beta^2 V_o = \frac{1}{\mu}\frac{\partial P_o}{\partial z} ,$$

or

$$\frac{\partial^2 V_o}{\partial r^2} + \frac{1}{r}\frac{\partial V_o}{\partial r} - \beta^2 V_o - \frac{1}{\mu}\frac{\partial P_o}{\partial z} = 0 \ . \tag{7}$$

When Equation (7) is substituted into Equation (6), the result is an expression for the equation of motion in terms of V_1 and P_1, including the interdependency term $\beta^2 V_1$, in the form

$$\frac{\partial^2 V_1}{\partial r^2} + \frac{1}{r}\frac{\partial V_1}{\partial r} - \left(\frac{i\omega}{\nu} + \beta^2\right) V_1 = \frac{1}{\mu}\frac{\partial P_1}{\partial z} \ . \tag{8}$$

Equations (3), (7) and (8) together provide a complete mathematical model for the analytical system shown in Fig. 6, subject to the eight restrictions upon which the development in this chapter is predicated. The work of Langhaar provides a solution to Equation (7) and permits the calculation of V_o, the steady-state velocity component in Equation (3), for any point (r, z) in a tube having a prescribed radius R and through which air flows at a prescribed Reynolds number based upon the mean velocity of the forced flow in the tube. An outline of Langhaar's solution development for Equation (6) and a summary of his numerical results are included in the Appendix. A solution to Equation (8) is the only additional requirement in Equation (3) for a complete determination of the z-component of velocity. The structure of Equation (8) indicates that there are two important cases which must be considered in the development of a solution to obtain an expression for V_1. The first case is the general condition at points in the analytical system where the effects of β cannot be neglected. The probable complexity of

the solution for this case suggests a limitation to the practical usefulness of the resultant expression for V_1 which might be severe. The second case includes the points in the system where the effects of β become negligible. Although the latter case probably offers the less complex solution, the practical usefulness of its solution depends upon the scope of application of the resultant expression for V_1.

CHAPTER III

SOLUTION OF THE MODEL FOR THE GENERAL CASE

An understanding of the variation of velocity and pressure as functions of axial location in an acoustically resonant tube is provided by the established theory for open organ pipes in resonance. The wave length λ_f for the fundamental resonant frequency of an open organ pipe is equal to twice the length of the pipe. Resonance will also be procuded by all the harmonics of this fundamental frequency ω_f, or at any $n\omega_f$, where n is any integer. Points of maximum particle disturbance and maximum velocity effects are established at the two open ends of the pipe and at points between the ends such that the spacing interval between successive loops is $\lambda/2$. The velocity vectors at successive loops are directed 180 degrees out of phase. The points which are half the distance between successive loops are termed nodes and are locations at which the particles remain undisturbed by the acoustic waves. The velocity due to acoustic vibrations at these nodal points is zero. Pressure effects are 90 degrees out of phase with the velocity effects such that a velocity loop is a "pressure node" and a velocity node is a "pressure loop".

A schematic diagram of these effects is shown in Fig. 7. The frequency of the vibrations determines the number of loops and nodes in the tube. As an example of this fact, Fig. 7 shows that the fundamental frequency of the tube, or where n = 1, produces two loops and one node since the length of the tube is $\lambda_f/2$. In this case and for

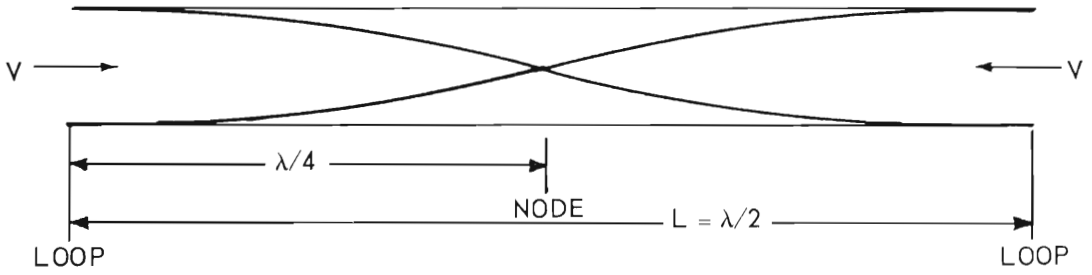

a. FUNDAMENTAL TUBE FREQUENCY, n = 1.

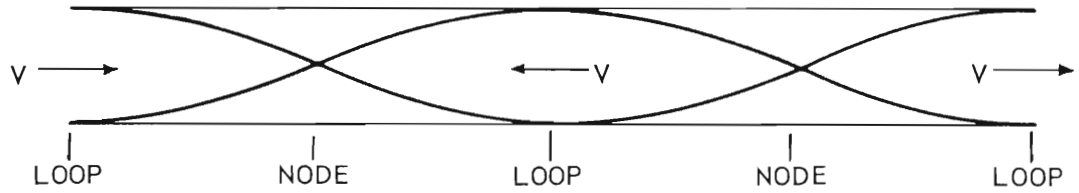

b. FIRST HARMONIC TUBE FREQUENCY, n = 2.

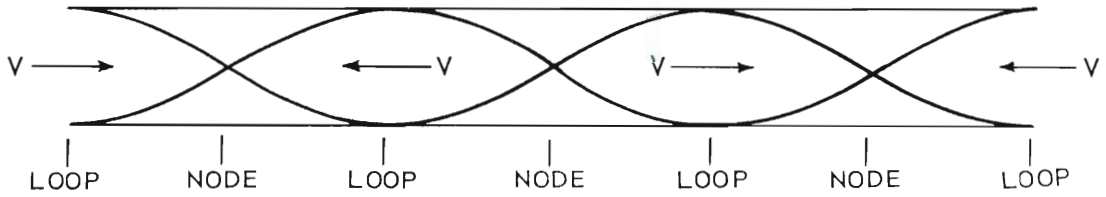

c. SECOND HARMONIC TUBE FREQUENCY, n = 3.

Figure 7. Schematic Representation of the Positions of Velocity Nodes and Loops in an Open Pipe for Various Resonant Frequencies.

all odd values of n, the velocity vectors at the tube ends are out of phase. For the case of resonance produced by the first harmonic frequency, or where n = 2, the length of the tube is now equal to the wave length of the sound waves such that three loops and two nodes are produced. In this case and for all even values of n, the velocity vectors at the tube ends are in phase.

Although the theory for open organ pipes designates the open ends as true velocity loops, this designation is not strictly correct. There is actually an escape of some of the sound energy at each reflection. This escape of energy excites the air beyond the open ends causing the "effective" length of the pipe to be somewhat greater than the actual length. For pipes whose lengths are considerably greater than their diameters, this departure from theory is not sufficiently significant to be of practical importance at relatively low sound-field frequencies. For this reason, the theoretical loop and node geometries were employed in the development described in this chapter.

The results of this analysis suggest that the velocities and pressures due to the resonant acoustic vibrations can be expressed as periodic functions of axial location in the form

$$V_l = v \cos(n\pi z/L) \tag{9}$$

and

$$P_l = iP_{max} \sin (n\pi z/L). \tag{10}$$

In Equation (9), v is the amplitude, or the maximum value of V_l at a given radius location, and is a function of the radial position r alone.

In Equation (10), P_{max} is the maximum pressure in the tube due to the acoustic vibrations and is constant for all r and z values. Equation (10) yields the expression

$$\frac{\partial P_1}{\partial z} = \frac{in\pi}{L} P_{max} \cos (n\pi z/L). \qquad (11)$$

The parameter P_{max} can be measured by means of a sound level meter which indicates the pressure resulting from the acoustic vibrations above a reference pressure level. The meter reading is in decibels. The measured value is termed the sound pressure level (SPL) and is defined by Peterson and Beranek (14) as

$$SPL = 20 \log \frac{\overline{P}}{P_{mr}} ,$$

where P_{mr} is the reference pressure for the particular sound level meter and $\overline{P}$ is the root-mean-square sound pressure in the same pressure units as P_{mr}. Then, since

$$\overline{P} = 0.707 P_{max}$$

for a given sound measurement, the relationship between P_{max} in Equation (11) and a measured value of SPL is

$$SPL = 20 \log \frac{(0.707)P_{max}}{P_{mr}} .$$

Therefore,

$$P_{max} = \frac{P_{mr}}{0.707} e^{SPL/8.68} ,$$

or, letting

$$P_r = \frac{P_{mr}}{0.707} ,$$

$$P_{max} = P_r \, e^{SPL/8.68} . \tag{12}$$

The substitution of Equation (12) into Equation (11) yields

$$\frac{\partial P_1}{\partial z} = \frac{in\pi}{L} P_r \, e^{SPL/8.68} \cos (n\pi z/L) . \tag{13}$$

The result of the combination of Equations (8), (9), and (13) is

$$\cos (n\pi z/L)\left[\frac{\partial^2 v}{\partial r^2} + \frac{1}{r}\frac{\partial v}{\partial r} - (i\omega/\nu + \beta^2)v\right] = \frac{in\pi}{L\mu} P_r e^{SPL/8.68} \cos (n\pi z/L). \tag{14}$$

For all values of cos (nπz/L) except zero, Equation (14) may be simplified to the form

$$\frac{\partial^2 v}{\partial r^2} + \frac{1}{r}\frac{\partial v}{\partial r} - (i\omega/\nu + \beta^2)v = \frac{in\pi}{L\mu} P_r e^{SPL/8.68} . \tag{15}$$

A particular solution for Equation (15) is

$$v = - \frac{i\alpha_1}{(\beta^2 + i\omega/\nu)} , \tag{16}$$

where

$$\alpha_1 = \frac{n\pi P_r e^{SPL/8.68}}{L\mu} . \tag{17}$$

The complementary equation

$$\frac{\partial^2 v}{\partial r^2} + \frac{1}{r}\frac{\partial v}{\partial r} + (- \beta^2 - i\omega/\nu)v = 0$$

has the form of the Bessel equation of zero order with a complex parameter. The only solution for this equation which is finite at r = 0 is

$$v = C_2 \, J_o\left[ir(\beta^2 + i\omega/\nu)^{1/2}\right] \quad . \tag{18}$$

The complex parameter in Equation (18) may be expressed as

$$\beta^2 + i\omega/\nu = p \, e^{i\Psi} \, ,$$

where

$$p = \left[\beta^4 + (\omega/\nu)^2\right]^{1/2} = \left|\beta^2 + i\omega/\nu\right| \, ,$$

and

$$\Psi = \tan^{-1} \, (\omega/\beta^2\nu) \, .$$

Then

$$i \, (\beta^2 + i\omega/\nu)^{1/2} = p^{1/2} \, e^{\frac{i(\Psi + \pi)}{2}} \, .$$

The entire argument of the Bessel function in Equation (18) may now be expressed in the polar complex form

$$ir \, (\beta^2 + i\omega/\nu)^{1/2} = qe^{i\varphi} \, , \tag{19}$$

where

$$q = rp^{1/2}$$

and

$$\varphi = (\psi + \pi)/2 \ .$$

The substitution of Equation (19) into Equation (18) yields the complementary solution for Equation (15) in the form

$$v = C_2 \ J_o \ (qe^{i\varphi}) \ . \tag{20}$$

The general solution for Equation (15) may now be written as

$$v = C_2 \ J_o \ (qe^{i\varphi}) - i\alpha_1/pe^{i\psi} \ . \tag{21}$$

The substitution of the boundary condition that $v = 0$ at $r = R$ into Equation (21) together with the representation $Rp^{1/2} = Q$ gives

$$C_2 = \frac{i\alpha_1}{pe^{i\psi} J_o \ (Qe^{i\varphi})} \ . \tag{22}$$

The combination of Equations (21) and (22) results in the expression

$$v = \frac{\alpha_1 e^{i\pi/2}}{pe^{i\psi}} \left[\frac{J_o \ (qe^{i\varphi}) - J_o \ (Qe^{i\varphi})}{J_o \ (Qe^{i\varphi})} \right] \ . \tag{23}$$

Values for the expression J_o with complex argument have been tabulated by the National Bureau of Standards (15). The values are expressed in the form $\mathcal{R} + i\mathcal{I}$ where $\mathcal{R}$ is the real part and $\mathcal{I}$ is the real-valued imaginary part of the evaluation. Tabulated entries are included for values of q from zero to ten and for values of φ in the first quadrant. Since expressions for this Bessel function for values of φ in the second quadrant will be of interest in the use of Equation (23),

the conversion expression given in the National Bureau of Standards tables is of value. This expression is

$$J_o(q,\varphi) = \mathcal{R}(q,\eta) - i\,\mathcal{I}(q,\eta) , \tag{24}$$

where η is an angle in the first quadrant for which values of $J_o(qe^{i\eta})$ are tabulated and $\varphi = \pi - \eta$. Therefore $\eta = \pi - \varphi$. For Values of q greater than ten, an approximation formula obtained from the asymptotic series for $J_o(z)$ may be used. An expression of this type is given by McLachlan (16) in the form

$$J_o(qe^{i\eta}) = (2/\pi qe^{i\eta})^{1/2} \cos(qe^{i\eta} - \pi/4) . \tag{25}$$

Equation (25) may also be expressed in the form given in the National Bureau of Standards tables, or

$$J_o(qe^{i\eta}) = \mathcal{R}(q,\eta) + i\,\mathcal{I}(q,\eta), \tag{26}$$

where

$$\mathcal{R}(q,\eta) = (2/\pi q)^{1/2} \{(\cos \eta/2)[\cos(q\cos\eta - \pi/4)\cosh(q\sin\eta)] - (\sin\eta/2)[\sin(q\cos\eta - \pi/4)\sinh(q\sin\eta)]\} , \tag{27}$$

and

$$\mathcal{I}(q,\eta) = -(2/\pi q)^{1/2}\{(\cos\eta/2)[\sin(q\cos\eta - \pi/4)\sinh(q\sin\eta)] + (\sin\eta/2)[\cos(q\cos\eta - \pi/4)\cosh(q\sin\eta)]\} . \tag{28}$$

In Equations (26), (27) and (28) as in Equation (24), $\mathcal{R}(q,\eta)$ is the real part of the expression for $J_o\,(qe^{i\eta})$ and $\mathcal{I}(q,\eta)$ is the real-valued imaginary part. Equation (24) may again be used to obtain an expression for $J_o\,(qe^{i\varphi})$ from Equations (27) and (28) in the form

$$J_o\,(qe^{i\varphi}) = \mathcal{R}(q,\eta) - i\,\mathcal{I}(q,\eta)$$

such that

$$J_o\,(Qe^{i\varphi}) = \mathcal{R}(Q,\eta) - i\,\mathcal{I}(Q,\eta)\ . \tag{29}$$

The substitution of Equations (24) and (29) into Equation (23) results in the expression

$$v = \frac{\alpha_1 e^{i\pi/2}}{pe^{i\Psi}}\left[\frac{\mathcal{R}(q,\eta) - i\,\mathcal{I}(q,\eta) - \mathcal{R}(Q,\eta) + i\,\mathcal{I}(Q,\eta)}{\mathcal{R}(Q,\eta) - i\,\mathcal{I}(Q,\eta)}\right]$$

which can be reduced to the form

$$v = (\alpha_1/p)e^{i\left(\frac{\pi}{2} - \Psi\right)}(\Gamma + i\Delta)\ , \tag{30}$$

where

$$\Gamma = \frac{\mathcal{R}(Q,\eta)[\,\mathcal{R}(q,\eta) - \mathcal{R}(Q,\eta)] - \mathcal{I}(Q,\eta)[\,\mathcal{I}(Q,\eta) - \mathcal{I}(q,\eta)]}{\mathcal{R}^2(Q,\eta) + \mathcal{I}^2(Q,\eta)}\ ,$$

and

$$\Delta = \frac{\mathcal{R}(Q,\eta)[\,\mathcal{I}(Q,\eta) - \mathcal{I}(q,\eta)] + \mathcal{I}(Q,\eta)[\,\mathcal{R}(q,\eta) - \mathcal{R}(Q,\eta)]}{\mathcal{R}^2(Q,\eta) + \mathcal{I}^2(Q,\eta)}\ .$$

The fact that

$$e^{i(\frac{\pi}{2} - \Psi)}(\Gamma + i\Delta) = \left[\cos\left(\frac{\pi}{2} - \Psi\right) + i \sin\left(\frac{\pi}{2} - \Psi\right)\right](\Gamma + i\Delta)$$

permits a further simplification of Equation (30) to

$$v = \frac{\alpha_1}{p}(X + i\,Y)\ , \tag{31}$$

where

$$X = \Gamma \cos\left(\frac{\pi}{2} - \Psi\right) - \Delta \sin\left(\frac{\pi}{2} - \Psi\right) \tag{32}$$

and

$$Y = \Delta \cos\left(\frac{\pi}{2} - \Psi\right) + \Gamma \sin\left(\frac{\pi}{2} - \Psi\right)\ . \tag{33}$$

The complete expression for V_1 is obtained by the combination of Equations (9) and (31) which yields

$$V_1 = \frac{\alpha_1}{p}(X + i\,Y)\cos\left(\frac{n\pi z}{L}\right)\ . \tag{34}$$

The condition for acoustic resonance to be present in the system requires that

$$\omega = n\omega_f \tag{35}$$

in Equation (34). By including Equation (35) and the definitions of α_1 and p in Equation (34), an expression is obtained for V_1 as a function of the important flow and acoustic parameters which exist in the general case described in Chapter II. This expression is

$$V_1 = \frac{n\pi P_r e^{SPL/8.68}}{L\mu\left[\beta^4 + \left(\frac{n\omega_f}{v}\right)^2\right]^{1/2}} (X + i\,Y) \cos\left(\frac{n\pi z}{L}\right) . \qquad (36)$$

The numerical evaluation of this solution for the general case is time-consuming due to the expressions for X and Y given in Equations (32) and (33) which, in addition, depend upon the relationships given in the expressions for Γ and Δ. This fact verifies the prediction made in Chapter II relating to the probable complexity of the solution for the general case. A need was thereby established for the investigation of the special case where the effects of β may be considered negligible. This suggested a study not only to obtain a less complicated expression for V_1 but also to determine the scope of the domain in the system defined by the special case.

CHAPTER IV

SOLUTION OF THE MODEL FOR THE SPECIAL CASE

The domain of application.--The determination of the scope of the domain in the analytical system defined by the special case where the effects of β may be considered negligible resulted from the consideration of complex-variable theory. The complex parameter in Equation (18) was represented in polar form in Chapter III as

$$\beta^2 + i\omega/\nu = p\, e^{i\Psi} , \tag{37}$$

where p is the absolute value of the complex parameter, or

$$p = \left[\beta^4 + (\omega/\nu)^2\right]^{1/2} = \left|\beta^2 + i\omega/\nu\right| , \tag{38}$$

and Ψ is the vector angle of the radius vector p, or

$$\Psi = \tan^{-1}(\omega/\beta^2\nu) . \tag{39}$$

The relationships expressed in Equations (37), (38) and (39) are represented schematically in Fig. 8. From this representation it can be seen that the condition for which β becomes negligible in the complex parameter is defined when the angle Ψ approaches a value of $\pi/2$ such that the projection of the radius vector p on the imaginary axis is essentially equal to p, or

$$p = p \sin\Psi \Big]_{\Psi \to \pi/2} = \omega/\nu . \tag{40}$$

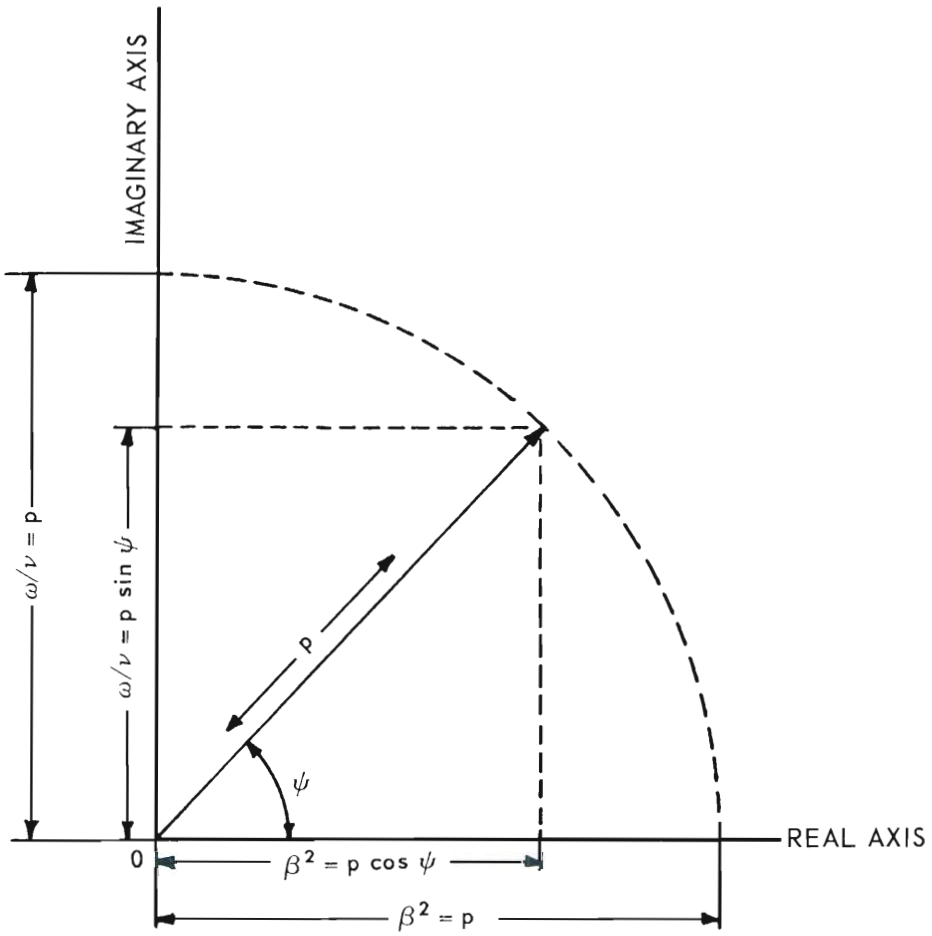

Figure 8. Schematic Diagram of the Polar Representation of the Complex Parameter in Equation (37).

From a consideration of orders of magnitude in Equation (38), the condition specified in Equation (40) will be satisfied, for all practical purposes, when

$$\beta^2 < 0.01\ (\omega/\nu)\ . \tag{41}$$

This fact becomes more apparent when Equations (39) and (41) are combined to give

$$\psi = \tan^{-1}\ (100) = 89^\circ\ 26'$$

and

$$\sin\ \psi = \sin\ (89^\circ\ 26') = 0.99995\ .$$

Then

$$\omega/\nu = p\ \sin\ \psi = 0.99995\ p\ ,$$

such that Equation (40) is satisfied within tolerable limits of approximation.

Equation (41) and the results of Langhaar which are summarized in the Appendix provide a method for the determination of the domain in a particular system in which the effects of β may be considered negligible. This method requires the specification of the tube length, tube radius, throughflow Reynolds number, mean air temperature and n for the resonant acoustic field in the tube. The tube length, mean air temperature and n provide values for ω and ν in Equation (41) from which a maximum negligible value of β can be calculated. The combination of this value of β and the specified values of tube radius and Reynolds number with

Langhaar's results yields the value of tube length z beyond which the effects of β are negligible in the analytical model. A particular numerical example of this procedure for the determination of the domain of the special case is given in Chapter V.

The solution development.---In the domain of the special case where β becomes negligible with respect to ω/ν, Equation (18) reduces to

$$v = C_2 \, J_o\left[ir(i\omega/\nu)^{1/2}\right] ,$$

which can be written

$$v = C_2 \, J_o\left[i^{3/2} r(\omega/\nu)^{1/2}\right] . \tag{42}$$

From the definition of Kelvin's ber and bei functions

$$J_o\left[i^{3/2} r(\omega/\nu)^{1/2}\right] = \text{ber } r(\omega/\nu)^{1/2} + i \text{ bei } r(\omega/\nu)^{1/2} .$$

The ber and bei functions can be expressed in the more convenient polar form such that

$$J_o\left[i^{3/2} r(\omega/\nu)^{1/2}\right] = M_o\left[r(\omega/\nu)^{1/2}\right] e^{i(\Theta_o)_r} \tag{43}$$

where

$$M_o\left[r(\omega/\nu)^{1/2}\right] = \left[\text{ber}^2 \, r(\omega/\nu)^{1/2} + \text{bei}^2 \, r(\omega/\nu)^{1/2}\right]^{1/2} \tag{44}$$

and

$$(\Theta_o)_r = \tan^{-1}\left[\frac{\text{bei } r(\omega/\nu)^{1/2}}{\text{ber } r(\omega/\nu)^{1/2}}\right] . \tag{45}$$

For this special case, Equation (16) can be written

$$v = - \frac{\alpha_1 i}{(i\omega/\nu)}$$

which reduces to

$$v = - \alpha_1 \nu/\omega \ . \tag{46}$$

The combination of Equations (42), (43) and (46) yields the general solution for the special case of negligible β in the form

$$v_s = C_2 \, M_o \left[r(\omega/\nu)^{1/2}\right] e^{i(\Theta_o)_r} - \alpha_1 \nu/\omega \tag{47}$$

where the subscript s refers to the special case. The substitution of the boundary condition that v = 0 at r = R into Equation (47) gives

$$C_2 = \frac{\alpha_1 \nu}{M_o \left[R(\omega/\nu)^{1/2}\right] e^{i(\Theta_o)_R}} \ , \tag{48}$$

where

$$M_o \left[R(\omega/\nu)^{1/2}\right] = \left[ber^2 R(\omega/\nu)^{1/2} + bei^2 R(\omega/\nu)^{1/2}\right]^{1/2}$$

and

$$(\Theta_o)_R = \tan^{-1} \left[\frac{bei \ R(\omega/\nu)^{1/2}}{ber \ R(\omega/\nu)^{1/2}}\right] .$$

The combination of Equations (47) and (48) gives

$$v_s = \alpha_1 \nu/\omega \left[\frac{M_o \left[r(\omega/\nu)^{1/2}\right]}{M_o \left[R(\omega/\nu)^{1/2}\right]} e^{i \left\{(\Theta_o)_r - (\Theta_o)_R\right\}} - 1\right] . \tag{49}$$

The angle $(\Theta_o)_r - (\Theta_o)_R$ is the phase of the ratio $M_o[r(\omega/\nu)^{1/2}]/M_o[R(\omega/\nu)^{1/2}]$ at any radius r relative to the ratio at the tube wall where r = R.

The complete expression for $(V_1)_s$ is obtained by the combination of Equations (9), (35) and (49) which yields

$$(V_1)_s = \alpha_1 \nu/n\omega_f \left[\frac{M_o[r(n\omega_f/\nu)^{1/2}]}{M_o[R(n\omega_f/\nu)^{1/2}]} e^{i\{(\Theta_o)_r - (\Theta_o)_R\}} - 1 \right] \cos(n\pi z/L). \quad (50)$$

When the definition of α_1 is included, the significant real part of Equation (50) becomes

$$(V_1)_s = \frac{\nu\pi P_r e^{SPL/8.68}}{L\mu\omega_f} \left[\frac{M_o[r(n\omega_f/\nu)^{1/2}]}{M_o[R(n\omega_f/\nu)^{1/2}]} \cos\{(\Theta_o)_r - (\Theta_o)_R\} - 1 \right] \cos(n\pi z/L) . \quad (51)$$

The numerical evaluation of Equation (51) is much less tedious and complicated than the evaluation of Equation (36). This fact gives greater practical significance to Equation (51) in the domain of its application. For purposes of numerical evaluation of Equation (51), the M_o ratio can be written in the form

$$\frac{M_o[r(n\omega_f/\nu)^{1/2}]}{M_o[R(n\omega_f/\nu)^{1/2}]} = \left[\frac{ber^2 r(n\omega_f/\nu)^{1/2} + bei^2 r(n\omega_f/\nu)^{1/2}}{ber^2 R(n\omega_f/\nu)^{1/2} + bei^2 R(n\omega_f/\nu)^{1/2}} \right]^{1/2} \quad (52)$$

which can be evaluated with greater facility. Values for ber and bei functions which have arguments less than ten are tabulated by McLachlan (16) who, in addition, gives approximation relationships for ber and bei functions whose arguments are greater than ten. These approximation

relationships, when expressed in terms of the arguments of the Bessel functions in Equation (52) take the forms

$$\text{ber } r(n\omega_f/\nu)^{1/2} \cong \frac{0.3989}{r^{1/2}(n\omega_f/\nu)^{1/4}} e^{r(n\omega_f/2\nu)^{1/2}} A_r \ , \tag{53}$$

where

$$A_r = \sin \left[40.514\ r(n\omega_f/\nu)^{1/2} + 67.5\right]^\circ \tag{54}$$

$$+ \frac{1}{8r(n\omega_f/\nu)^{1/2}} \sin \left[40.514\ r(n\omega_f/\nu)^{1/2} + 22.5\right]^\circ \ ,$$

and

$$\text{bei } r(n\omega_f/\nu)^{1/2} \cong \frac{0.3989}{r^{1/2}(n\omega_f/\nu)^{1/4}} e^{r(n\omega_f/2\nu)^{1/2}} B_r \ , \tag{55}$$

where

$$B_r = \sin \left[40.514\ r(n\omega_f/\nu)^{1/2} - 22.5\right]^\circ \tag{56}$$

$$+ \frac{1}{8r(n\omega_f/\nu)^{1/2}} \sin \left[40.514\ r(n\omega_f/\nu)^{1/2} - 67.5\right]^\circ \ .$$

The combination of Equations (45), (53) and (55) yields the expression

$$\Theta_o(r) = \tan^{-1} (B_r/A_r) \tag{57}$$

for values of $r(n\omega_f/\nu)^{1/2}$ greater than ten.

A very important additional value of the expression for $(V_l)_s$ expressed in Equation (51) arises from the fact that the domain of the

special case includes the entire analytical system under conditions of no throughflow. In the absence of throughflow, β and V_o become zero and Equation (51) becomes an expression for the entire velocity effects in the system. Although the investigations of Reyleigh (1), Andrade (2), Jackson and Johnson (3) and Meyer and Güth (4) pertain to closed-tube systems, the results of these investigations provide an interesting comparison with the results obtained from Equation (51) for an open-tube system. It would be expected that some similarities should exist between the closed system and the open system with no throughflow.

CHAPTER V

RESULTS OF NUMERICAL EVALUATION

The selection of numerical values for the various parameters in the solutions derived for the analytical model was based upon typical values for these parameters encountered in the experimental investigations which are summarized in Chapter I. The numerical evaluation of the analytical velocity expressions using values for the parameters which are within the range of typical experimental values for these parameters provided a possibility for a comparison between analytical and observed results. A convenient tube length L of four feet was selected. The average temperature and pressure of the air which occupies the tube were taken as approximately 300°F and one atmosphere, respectively. At this temperature the following values for the pertinent air properties are given by Kreith (17):

$$\nu = 3 \times 10^{-4} \text{ ft}^2/\text{sec} ;$$

$$\mu = 1.6 \times 10^{-5} \text{ lb}_m/\text{ft-sec}.$$

For a tube with a length of four feet, the fundamental resonant frequency ω_f is approximately 865 radians per second.

In addition to these fixed parameter values, values for the tube radius R, the acoustic harmonic parameter n, the throughflow Reynolds number, and the sound pressure level were varied over selected ranges to determine the effects of these variable parameters on the velocity

distribution in the system. The selected values for R were 0.058 ft, 0.116 ft and 0.174 ft. Values for the Reynolds number of 100, 1000 and 2000 were considered to be representative of the laminar regime. The fundamental, first harmonic, third harmonic and seventh harmonic frequencies for the system for which n = 1, 2, 4 and 8, respectively, were considered. Finally, sound pressure levels of 140 decibels, 145 decibels, 150 decibels, 155 decibels and 160 decibels were selected. These values for the designated parameters establish numerically-specified examples of the analytical model for which particular numerical solutions of the velocity expressions derived in Chapters III and IV can be computed. The determination of a numerical value for the velocity at a particular point (r, z) in the system requires the determination of the appropriate velocity expression for this point. Obviously, the expression for $(V_1)_s$ cannot be employed at a point in the system where β is not negligible.

Determination of the domain of the special case.--The domains of the special case of negligible β in the particular systems defined by the various combinations of the prescribed numerical values of the system parameters were determined by consideration of orders of magnitude. For these systems, the minimum value of the expression ω/ν occurs when ω is the fundamental frequency ω_f. Thus

$$(\omega/\nu)_{minimum} = \omega_f/\nu = 865/(3 \times 10^{-4}), \text{ or}$$

$$(\omega/\nu)_{minimum} = 2.88 \times 10^{6} \text{ ft}^{-2} .$$

The condition for negligible β given by Equation (41) prescribes that

the velocity expression for the special case is applicable at all points in the particular systems considered in this study where

$$\beta^2 < (0.01)(2.88 \times 10^6) \text{ , or}$$

$$\beta < 170 \text{ .}$$

Even larger values of β are negligible in systems operating at frequencies greater than the fundamental frequency.

From an examination of Langhaar's results it is evident that the magnitude of β for a particular system depends upon the tube radius R and the throughflow Reynolds number. Maximum values of axial position in the tube beyond which β is negligible can be determined when R and Re are specified. As an example of this important fact, when R is 0.058 ft and the throughflow Reynolds number is 100, the product of the maximum negligible value of β, or β_{max}, and R becomes

$$\beta_{max} R = (170)(0.058) \text{ , or}$$

$$\beta_{max} R = 9.86 \text{ .}$$

From Langhaar's results, which are summarized in the Appendix, this value of βR corresponds to a value of $2z/R\text{Re}$ equal to 0.0038; therefore, the value of z corresponding to the prescribed values of R, Re and β_{max} is 0.011 ft, or 0.132 in. Thus, in a tube with a length of four feet, a radius of 0.058 ft and a throughflow Reynolds number of 100, the effects of β on V_1 are negligible at all values of z/L greater than 0.011/4, or 0.0028. Values for z_m and $(z/L)_{min}$ beyond which the effects of β on V_1 are negligible in a tube four feet long were calculated for various

values of tube radius and throughflow Reynolds number. The results of these calculations are given in Table 1 and Fig. 9.

Determination of the values of $(V_1)_s$ at r = 0.--The expression for $(V_1)_s$ at the tube centerline is an adaptation of Equation (51) which can be written in the form

$$(V_1)_{s,0} = \frac{\nu\pi P_r e^{SPL/8.68}}{L\mu\omega_f}\left[\frac{1 - \cos\,(\Theta_o)_R}{M_o\left[R(n\omega_f/\nu)^{1/2}\right]} - 1\right] \cos\,(n\pi z/L) \ . \qquad (58)$$

For all values of $R(n\omega_f/\nu)^{1/2}$ greater than ten, Equations (44), (53) and (55) can be combined to give a sufficiently accurate approximation relationship for $M_o\left[R(n\omega_f/\nu)^{1/2}\right]$ in the form

$$M_o\left[R(n\omega_f/\nu)^{1/2}\right] = 0.3989\left[\frac{A_R^2 + B_R^2}{R(n\omega_f/\nu)^{1/2}}\right]^{1/2} e^{R(n\omega_f/2\nu)^{1/2}} \ . \qquad (59)$$

Since the smallest value of $R(n\omega_f/\nu)^{1/2}$ resulting from the combination of the selected values of R, n, ω_f and ν is

$$\left[R(n\omega_f/\nu)^{1/2}\right]_{min} = (0.058)(2.88 \times 10^6)^{1/2} \ , \text{ or}$$

$$\left[R(n\omega_f/\nu)^{1/2}\right]_{min} \cong 100 \ ,$$

Equations (58) and (59) were combined to give an expression for $(V_1)_{s,0}$ applicable to the entire range of values selected for the parameters of the system. Values of $(V_1)_{s,0}$ were calculated for various combinations of the selected values for R, n and SPL from this expression. The calculations were performed by an IBM 650 Digital Computer. The results

Table 1. Results of Calculations to Determine the Domain of the Special Case in a Tube Four Feet Long

Re	R,ft	$\beta_{max}R$	RRe,ft	z_m,ft	z_m,ins	z/L
100	0.05	8.5	5	0.015	0.180	0.00375
	0.10	17.0	10	0.006	0.072	0.00150
	0.14	23.8	14	0.004	0.048	0.00100
	0.18	30.6	18	0.003	0.036	0.00075
1000	0.05	8.5	50	0.150	1.80	0.0375
	0.10	17.0	100	0.060	0.72	0.0150
	0.14	23.8	140	0.040	0.48	0.0100
	0.18	30.6	180	0.030	0.36	0.0075
2000	0.05	8.5	100	0.300	3.60	0.0750
	0.10	17.0	200	0.120	1.44	0.0300
	0.14	23.8	280	0.080	0.96	0.0200
	0.18	30.6	360	0.060	0.72	0.0150

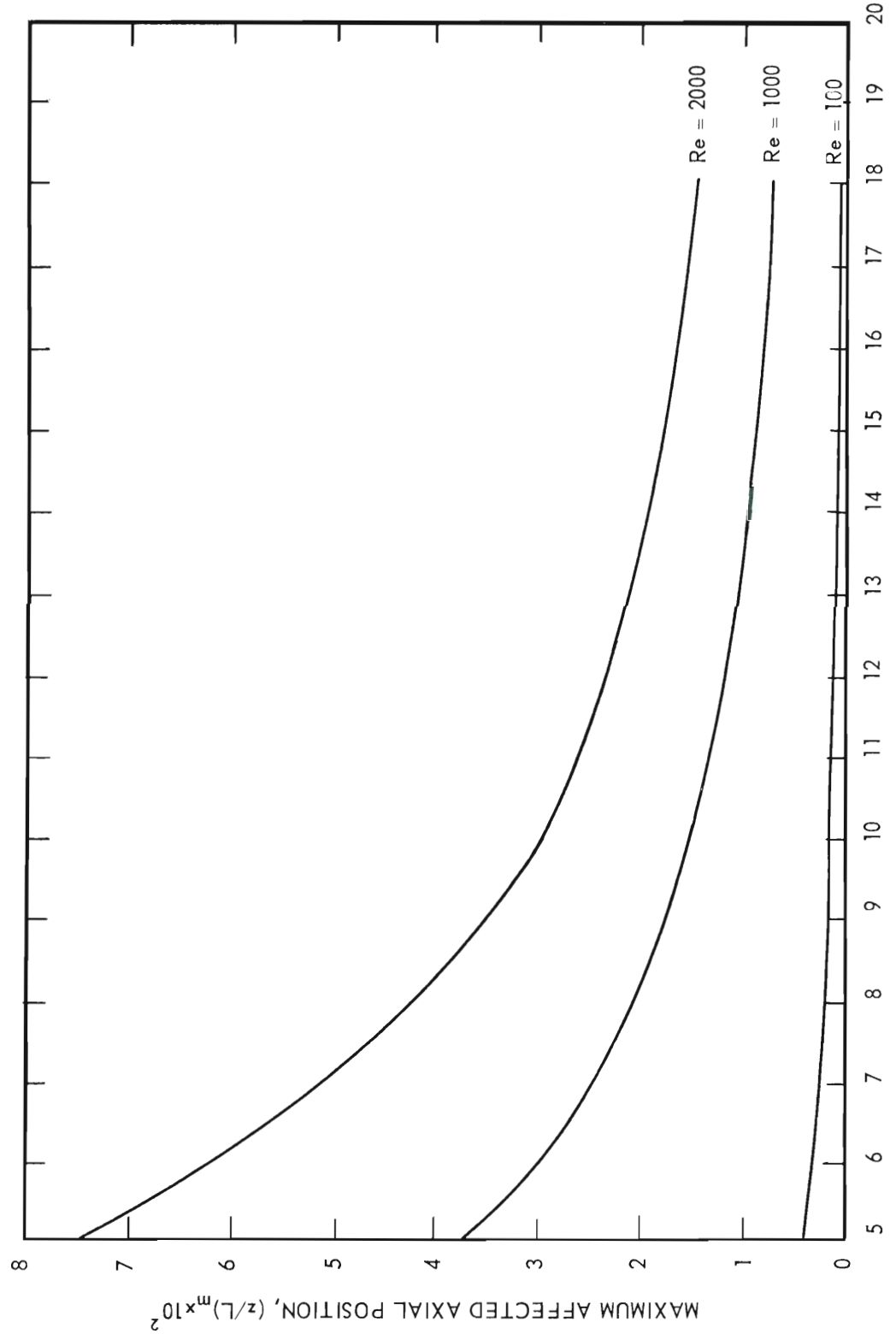

Figure 9. The Effect of Tube Radius and Throughflow Reynolds Number on the Scope of the Domain of the Special Case in a Resonant Tube Four Feet Long.

of this calculation procedure established the important fact that for the selected values of tube radius the term

$$\frac{1 - \cos\,(\Theta_o)_R}{M_o\left[R(n\omega_f/\nu)^{1/2}\right]}$$

in Equation (58) becomes negligible with respect to unity. This can be explained by the large value of the exponential term in the numerator of Equation (59). The expression for the combination of Equations (58) and (59) was then simplified to the form

$$(V_1)_{s,0} = -\frac{\nu\pi P_r e^{SPL/8.68}}{L\mu\omega_f}\cos\,(n\pi z/L)\ . \qquad (60)$$

Equation (60) is applicable for all combinations of values for R, n, ω_f and ν which make the exponential term in Equation (59) sufficiently large. The results of the calculation procedure for the determination of $(V_1)_{s,0}$ for the selected values of the various parameters are given in Tables 2 through 5 and Figs. 10 through 13.

Determination of the value of $(V_1)_s$ at any point (r,z).--The determination of the velocity profile in the domain of the special case requires the evaluation of Equation (51). The approximation relationships expressed in Equations (53) and (55) may be used in the evaluation of Equation (51) when the values of $r(n\omega_f/\nu)^{1/2}$ and $R(n\omega_f/\nu)^{1/2}$ are greater than ten. For the selected values of n, ω_f, ν and R it has already been shown that $R(n\omega_f/\nu)^{1/2}$ will be greater than ten. If, in addition, values of r no smaller than (0.1)R are used in the evaluation of Equation (51), the values of $r(n\omega_f/\nu)^{1/2}$ will also be greater than

Table 2. Values of $(V_1)_{s,0}$ Calculated from Equation (60); n = 1

z/L	$(V_1)_{s,0} = (V_1)_s$ at Tube Centerline, ft/sec				
SPL :	140 db	145 db	150 db	155 db	160 db
1.00	0.101	0.181	0.321	0.572	1.016
0.75	0.072	0.128	0.227	0.404	0.721
0.50	0.000	0.000	0.000	0.000	0.000
0.25	-0.072	-0.128	-0.227	-0.404	-0.721
0.00	-0.101	-0.181	-0.321	-0.572	-1.016

Table 3. Values of $(V_1)_{s,0}$ Calculated from Equation (60); n = 2

z/L	$(V_1)_{s,0} = (V_1)_s$ at Tube Centerline, ft/sec				
SPL :	140 db	145 db	150 db	155 db	160 db
1.000	-0.101	-0.181	-0.321	-0.572	-1.016
0.875	-0.072	-0.128	-0.227	-0.404	-0.721
0.750	0.000	0.000	0.000	0.000	0.000
0.625	0.072	0.128	0.227	0.404	0.721
0.500	0.101	0.181	0.321	0.572	1.016
0.375	0.072	0.128	0.227	0.404	0.721
0.250	0.000	0.000	0.000	0.000	0.000
0.125	-0.072	-0.128	-0.227	-0.404	-0.721
0.000	-0.101	-0.181	-0.321	-0.572	-1.016

Table 4. Values of $(V_l)_{s,0}$ Calculated from Equation (60); n = 4

z/L	$(V_l)_{s,0} = (V_l)_s$ at Tube Centerline, ft/sec				
SPL :	140 db	145 db	150 db	155 db	160 db
1.0000	-0.101	-0.181	-0.321	-0.572	-1.016
0.9375	-0.072	-0.128	-0.227	-0.404	-0.721
0.8750	0.000	0.000	0.000	0.000	0.000
0.8125	0.072	0.128	0.227	0.404	0.721
0.7500	0.101	0.181	0.321	0.572	1.016
0.6875	0.072	0.128	0.227	0.404	0.721
0.6250	0.000	0.000	0.000	0.000	0.000
0.5625	-0.072	-0.128	-0.227	-0.404	-0.721
0.5000	-0.101	-0.181	-0.321	-0.572	-1.016
0.4375	-0.072	-0.128	-0.227	-0.404	-0.721
0.3750	0.000	0.000	0.000	0.000	0.000
0.3125	0.072	0.128	0.227	0.404	0.721
0.2500	0.101	0.181	0.321	0.572	1.016
0.1875	0.072	0.128	0.227	0.404	0.721
0.1250	0.000	0.000	0.000	0.000	0.000
0.0625	-0.072	-0.128	-0.227	-0.404	-0.721
0.0000	-0.101	-0.181	-0.321	-0.572	-1.016

Table 5. Values of $(V_l)_{s,0}$ Calculated from Equation (60); n = 8

z/L	$(V_l)_{s,0} = (V_l)_s$ at Tube Centerline, ft/sec				
SPL :	140 db	145 db	150 db	155 db	160 db
1.00000	-0.101	-0.181	-0.321	-0.572	-1.016
0.96875	-0.072	-0.128	-0.227	-0.404	-0.721
0.93750	0.000	0.000	0.000	0.000	0.000
0.90625	0.072	0.128	0.227	0.404	0.721
0.87500	0.101	0.181	0.321	0.572	1.016
0.84375	0.072	0.128	0.227	0.404	0.721
0.81250	0.000	0.000	0.000	0.000	0.000
0.78125	-0.072	-0.128	-0.227	-0.404	-0.721
0.75000	-0.101	-0.181	-0.321	-0.572	-1.016
0.71875	-0.072	-0.128	-0.227	-0.404	-0.721
0.68750	0.000	0.000	0.000	0.000	0.000
0.65625	0.072	0.128	0.227	0.404	0.721
0.62500	0.101	0.181	0.321	0.572	1.016
0.59375	0.072	0.128	0.227	0.404	0.721
0.56250	0.000	0.000	0.000	0.000	0.000
0.53125	-0.072	-0.128	-0.227	-0.404	-0.721
0.50000	-0.101	-0.181	-0.321	-0.572	-1.016
0.46875	-0.072	-0.128	-0.227	-0.404	-0.721
0.43750	0.000	0.000	0.000	0.000	0.000
0.40625	0.072	0.128	0.227	0.404	0.721
0.37500	0.101	0.181	0.321	0.572	1.016
0.34375	0.072	0.128	0.227	0.404	0.721
0.31250	0.000	0.000	0.000	0.000	0.000
0.28125	-0.072	-0.128	-0.227	-0.404	-0.721
0.25000	-0.101	-0.181	-0.321	-0.572	-1.016
0.21875	-0.072	-0.128	-0.227	-0.404	-0.721
0.18750	0.000	0.000	0.000	0.000	0.000
0.15625	0.072	0.128	0.227	0.404	0.721
0.12500	0.101	0.181	0.321	0.572	1.016
0.09375	0.072	0.128	0.227	0.404	0.721
0.06250	0.000	0.000	0.000	0.000	0.000
0.03125	-0.072	-0.128	-0.227	-0.404	-0.721
0.00000	-0.101	-0.181	-0.321	-0.572	-1.016

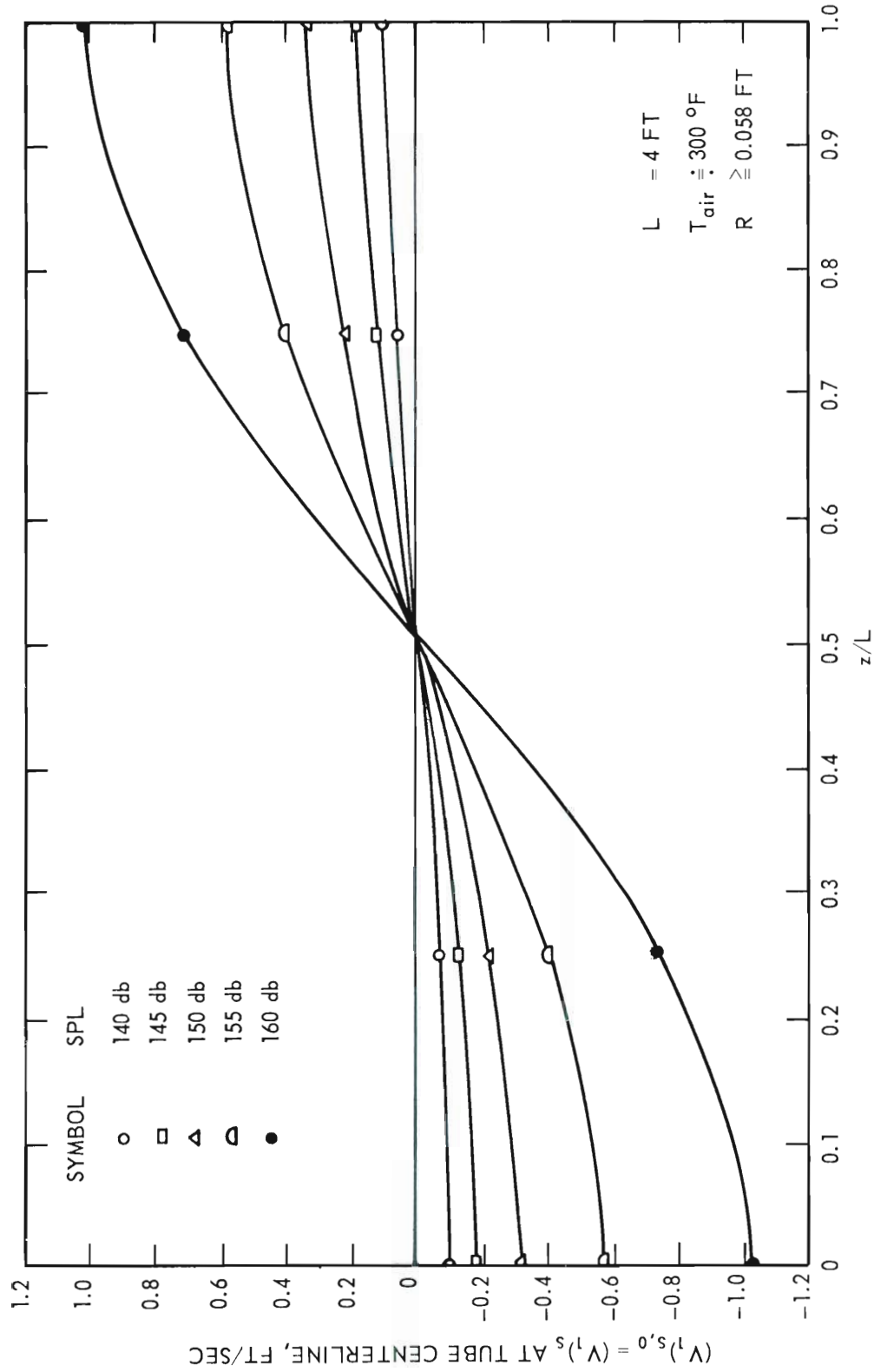

Figure 10. Tube Centerline Velocity for the Special Case as a Function of Axial Tube Position and Sound Pressure Level for the Fundamental Tube Frequency.

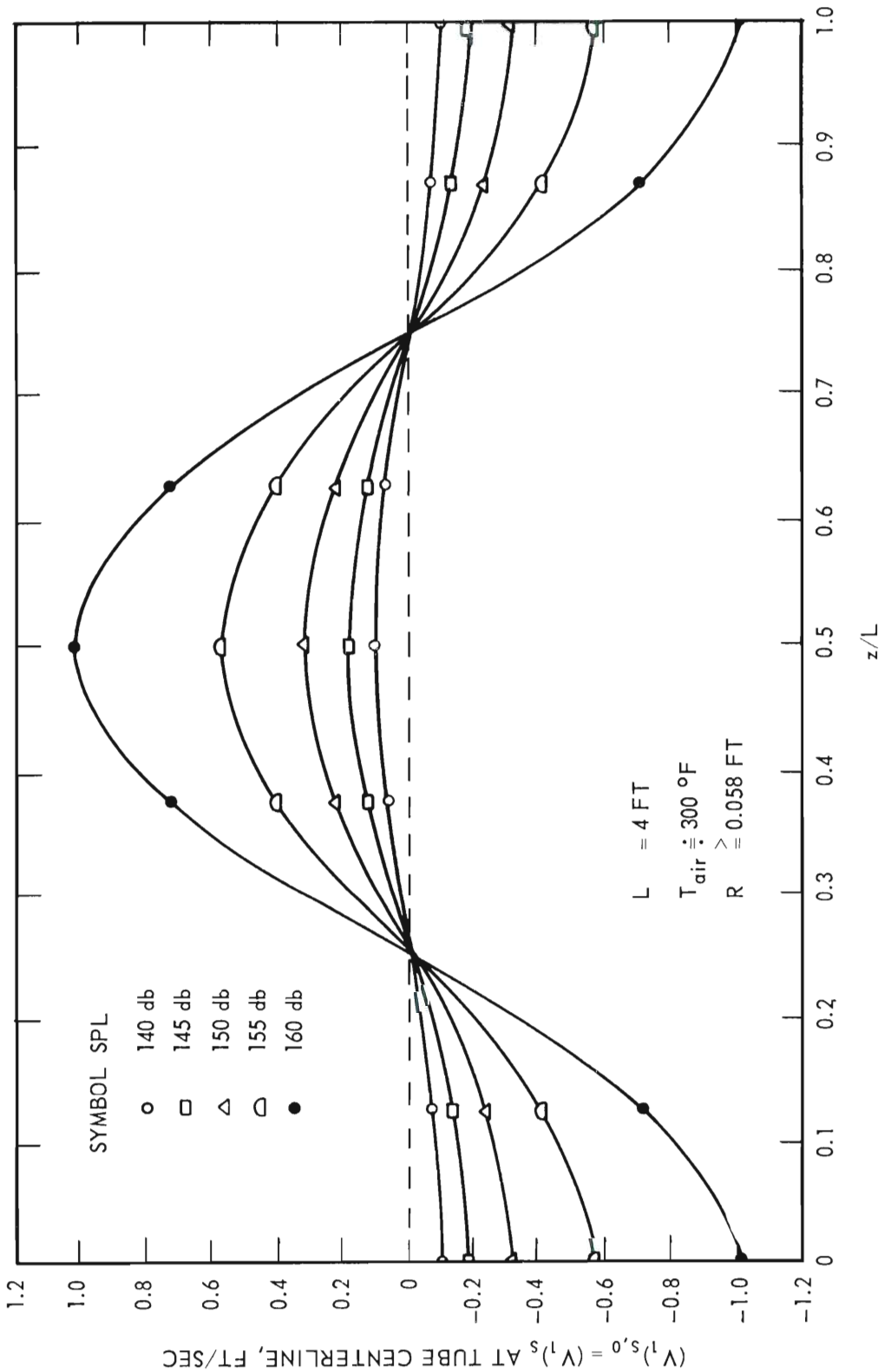

Figure 11. Tube Centerline Velocity for the Special Case as a Function of Axial Tube Position and Sound Pressure Level for the First Harmonic Tube Frequency.

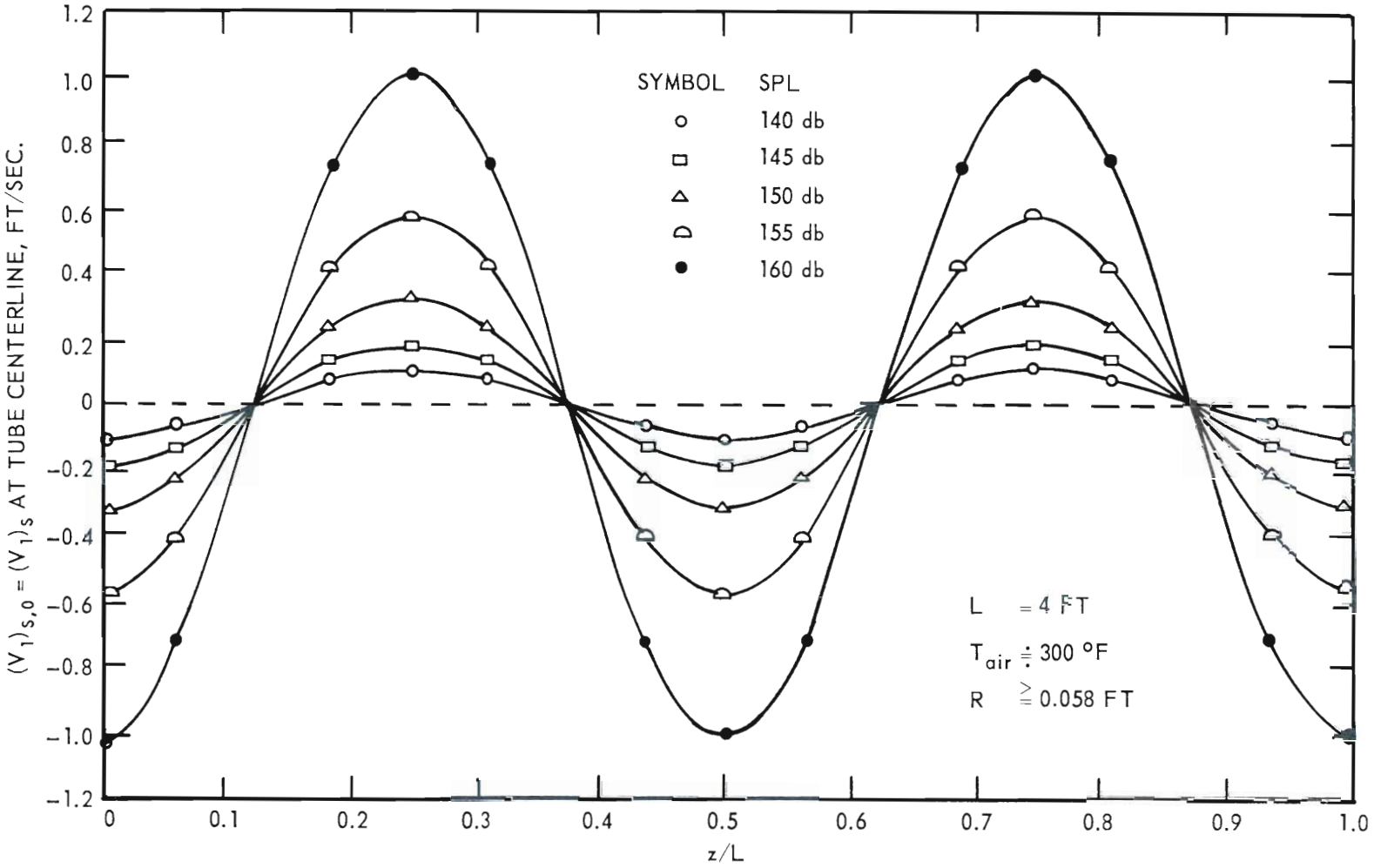

Figure 12. Tube Centerline Velocity for the Special Case as a Function of Axial Tube Position and Sound Pressure Level for the Third Harmonic Tube Frequency.

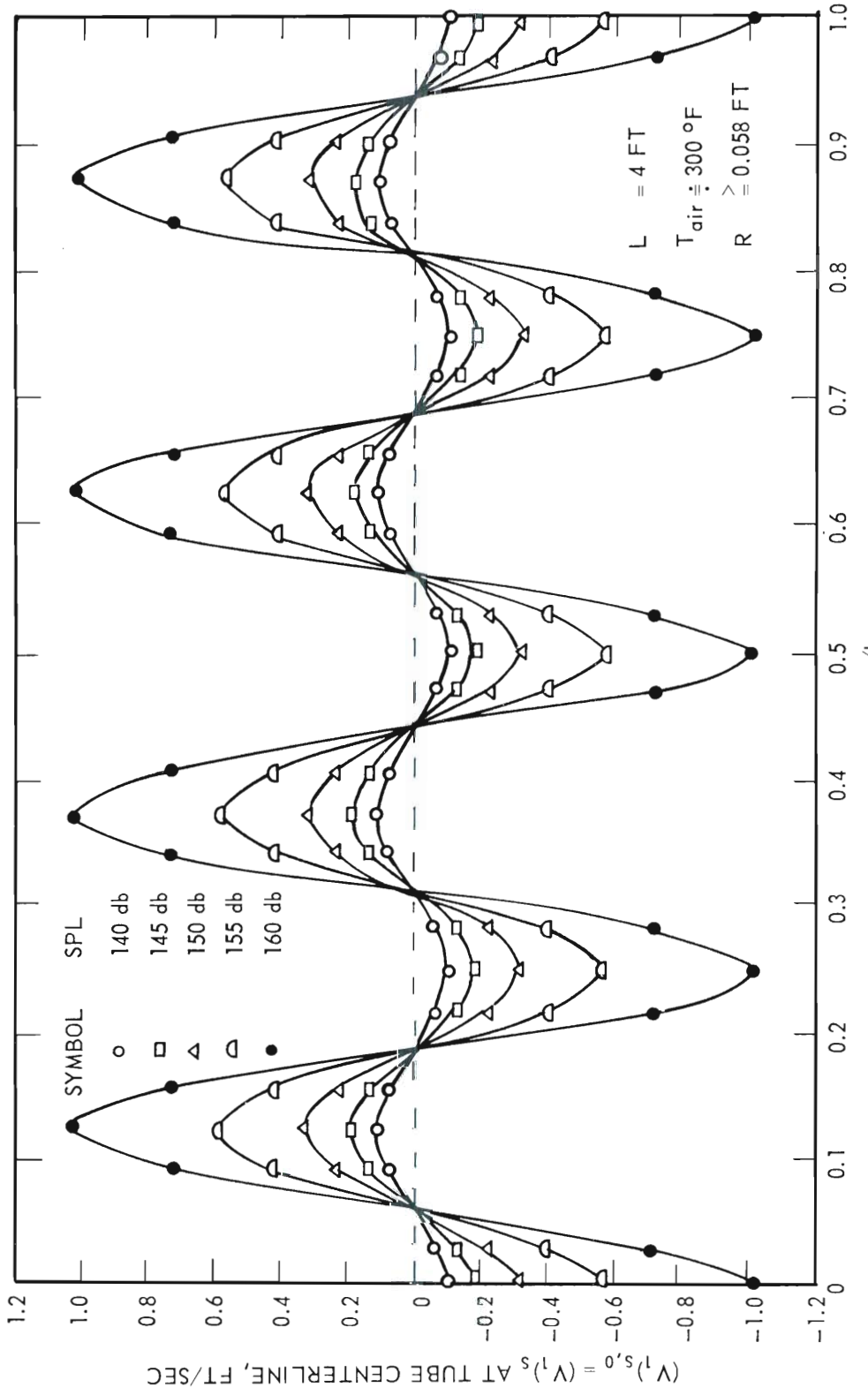

Figure 13. Tube Centerline Velocity for the Special Case as a Function of Axial Tube Position and Sound Pressure Level for the Seventh Harmonic Tube Frequency.

ten such that the approximation relationships can be used.

The most convenient procedure for the determination of $(V_1)_s$ at any point (r,z) provides for the evaluation of the ratio of $(V_1)_s$ at the prescribed point and $(V_1)_{s,0}$ at the same value of z. This procedure is facilitated by the combination of Equations (51) and (60) to yield

$$(V_1)_s/(V_1)_{s,0} = 1 - \frac{M_o\left[r(n\omega_f/\nu)^{1/2}\right]}{M_o\left[R(n\omega_f/\nu)^{1/2}\right]} \cos\left\{(\Theta_o)_r - (\Theta_o)_R\right\} . \qquad (61)$$

When the approximation relationships Equations (53) and (55) are included in Equation (61), the resultant expression is

$$\frac{(V_1)_s}{(V_1)_{s,0}} = 1 - \left[\frac{R(A_r^2 + B_r^2)}{r(A_R^2 + B_R^2)}\right]^{1/2} e^{(r-R)(2n\omega_f/\nu)^{1/2}/2} \cos\left\{(\Theta_o)_r - (\Theta_o)_R\right\} . \qquad (62)$$

Equation (62) was evaluated on an IBM 650 Digital Computer for various values of R, n and r. The results of this evaluation procedure are given in Tables 6 through 8 and Figs. 14 through 19.

Determination of the value of $(U_1)_s$ at any point (r,z).--The radial component of velocity at any point in the domain of the special case was important in the determination of the velocity vector resultant at a point in the system. It is this vector which influences the direction of particle displacement in the acoustic field. The results of the evaluation of $(V_1)_s$ shown in Figs. 17, 18 and 19 clearly indicate that the velocity profile for $(V_1)_s$ is uniform across the central 90 per cent of the tube radius. The derivation of an expression for $(U_1)_s$ was simplified by using the results of the evaluation of $(V_1)_s$. The cross-section

Table 6. Calculated Values of $(V_l)_s/(V_l)_{s,0}$ for a Tube Radius of 0.058 ft

r/R	r	y = R-r	$(V_l)_s/(V_l)_{s,0}$			
	ft	mm	n: 1	2	4	8
0.100	0.0058	15.90	1.0000	1.0000	1.0000	1.0000
0.200	0.0116	14.14	1.0000	1.0000	1.0000	1.0000
0.300	0.0174	12.36	1.0000	1.0000	1.0000	1.0000
0.400	0.0232	10.60	1.0000	1.0000	1.0000	1.0000
0.500	0.0290	8.84	1.0000	1.0000	1.0000	1.0000
0.600	0.0348	7.07	1.0000	1.0000	1.0000	1.0000
0.700	0.0406	5.31	1.0000	1.0000	1.0000	1.0000
0.800	0.0464	3.54	0.9999	1.0000	1.0000	1.0000
0.900	0.0522	1.77	0.9992	0.9999	0.9999	1.0000
0.910	0.0528	1.58	0.9980	0.9999	0.9999	1.0000
0.920	0.0534	1.40	0.9969	1.0000	1.0000	0.9999
0.930	0.0539	1.25	1.0014	0.9991	0.9999	1.0000
0.940	0.0545	1.07	0.9921	0.9974	1.0000	0.9999
0.950	0.0551	0.89	0.9703	1.0017	0.9993	0.9999
0.960	0.0557	0.70	0.9407	0.9863	1.0030	0.9999
0.970	0.0563	0.52	0.9370	0.9478	0.9922	0.9974
0.980	0.0568	0.37	0.9566	1.0555	0.9413	0.9864
0.990	0.0574	0.18	0.6163	0.7932	0.9568	0.9447
0.992	0.0575	0.15	0.5122	0.6785	0.8556	0.9980
0.994	0.0577	0.09	0.3966	0.5391	0.7090	1.1157
0.996	0.0578	0.06	0.2709	0.3762	0.5131	0.6792
0.998	0.0579	0.03	0.1376	0.1939	0.2716	0.3768
1.000	0.0580	0.00	0.0000	0.0000	0.0000	0.0000

Table 7. Calculated Values of $(V_l)_s/(V_l)_{s,0}$ for a Tube Radius of 0.116 ft

r/R	r	y = R-r	$(V_l)_s/(V_l)_{s,0}$			
	ft	mm	n: 1	2	4	8
0.100	0.0116	31.80	1.0000	1.0000	1.0000	1.0000
0.200	0.0232	28.30	1.0000	1.0000	1.0000	1.0000
0.300	0.0348	24.72	1.0000	1.0000	1.0000	1.0000
0.400	0.0464	21.21	1.0000	1.0000	1.0000	1.0000
0.500	0.0580	17.67	1.0000	1.0000	1.0000	1.0000
0.600	0.0696	14.14	1.0000	1.0000	1.0000	1.0000
0.700	0.0812	10.60	1.0000	1.0000	1.0000	1.0000
0.800	0.0928	7.07	1.0000	1.0000	1.0000	1.0000
0.900	0.1044	3.54	0.9999	1.0000	1.0000	1.0000
0.910	0.1056	3.17	0.9999	1.0000	1.0000	1.0000
0.920	0.1068	2.81	1.0000	0.9999	1.0000	1.0000
0.930	0.1078	2.50	0.9999	1.0000	1.0000	1.0000
0.940	0.1090	2.13	1.0000	0.9999	1.0000	1.0000
0.950	0.1102	1.77	0.9993	0.9999	1.0000	1.0000
0.960	0.1114	1.40	1.0030	0.9999	0.9999	0.9999
0.970	0.1126	1.04	0.9922	0.9974	0.9999	0.9999
0.980	0.1136	0.73	0.9413	0.9864	0.9970	0.9999
0.990	0.1148	0.37	0.9568	0.9447	0.9416	1.0135
0.991	0.1150	0.31	0.9115	0.9649	0.9336	0.9734
0.992	0.1151	0.27	0.8556	0.9980	0.9333	0.9570
0.993	0.1152	0.24	0.7884	1.0472	0.9463	0.9407
0.994	0.1153	0.21	0.7090	1.1157	0.9801	0.9322
0.995	0.1155	0.15	0.6172	1.2063	1.0431	0.9449
0.996	0.1156	0.12	0.5131	0.6792	1.1441	0.9980
0.997	0.1157	0.09	0.3975	0.5398	0.7094	1.1156
0.998	0.1158	0.06	0.2716	0.3768	0.5136	1.3205
0.999	0.1159	0.03	0.1380	0.1943	0.2720	0.3771
1.000	0.1160	0.00	0.0000	0.0000	0.0000	0.0000

Table 8. Calculated Values of $(V_l)_s/(V_l)_{s,0}$ for a Tube Radius of 0.174 ft

r/R	r	y = R-r	$(V_l)_s/(V_l)_{s,0}$			
	ft	mm	n: 1	2	4	8
0.100	0.0174	47.75	1.0000	1.0000	1.0000	1.0000
0.200	0.0348	42.50	1.0000	1.0000	1.0000	1.0000
0.300	0.0522	37.15	1.0000	1.0000	1.0000	1.0000
0.400	0.0696	31.85	1.0000	1.0000	1.0000	1.0000
0.500	0.0870	26.55	1.0000	1.0000	1.0000	1.0000
0.600	0.1044	21.25	1.0000	1.0000	1.0000	1.0000
0.700	0.1218	15.91	1.0000	1.0000	1.0000	1.0000
0.800	0.1392	10.62	1.0000	1.0000	1.0000	1.0000
0.900	0.1566	5.31	1.0000	1.0000	1.0000	1.0000
0.910	0.1584	4.76	1.0000	1.0000	1.0000	1.0000
0.920	0.1602	4.21	1.0000	1.0000	1.0000	1.0000
0.930	0.1617	3.75	0.9999	0.9999	1.0000	1.0000
0.940	0.1635	3.20	0.9999	1.0000	1.0000	1.0000
0.950	0.1653	2.65	1.0000	0.9999	1.0000	1.0000
0.960	0.1671	2.10	0.9999	0.9999	1.0000	1.0000
0.970	0.1689	1.55	0.9980	0.9999	0.9999	1.0000
0.980	0.1704	1.10	1.0077	0.9974	1.0000	0.9999
0.990	0.1722	0.55	0.9376	0.9484	0.9923	0.9974
0.991	0.1724	0.49	0.9525	0.9373	0.9811	0.9971
0.992	0.1726	0.43	0.9801	0.9322	0.9652	0.9997
0.993	0.1728	0.37	1.0242	1.0613	0.9472	1.0086
0.994	0.1730	0.31	1.0884	1.0351	0.9337	1.0265
0.995	0.1731	0.27	1.1763	0.9796	1.0622	0.9485
0.996	0.1733	0.21	1.1291	0.8844	1.0199	0.9323
0.997	0.1735	0.15	1.4330	0.7398	0.9117	0.9650
0.998	0.1737	0.09	1.6022	0.5400	0.7096	1.1155
0.999	0.1738	0.06	0.2058	0.2878	0.3981	1.4597
1.000	0.1740	0.00	0.0000	0.0000	0.0000	0.0000

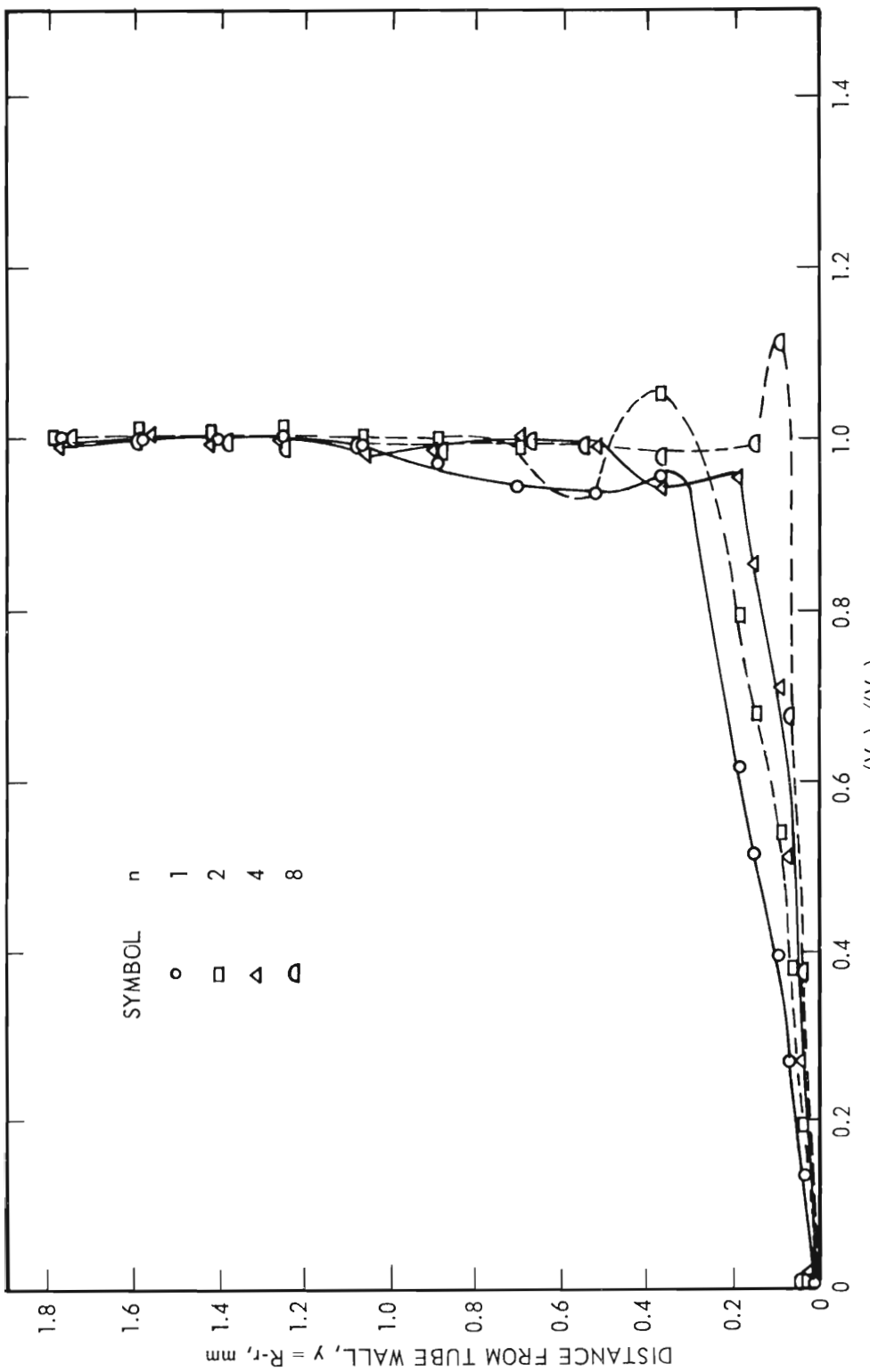

Figure 14. Velocity Profile Without Throughflow at a Point in the Domain of the Special Case as a Function of Sound Field Frequency; R = 0.058 ft.

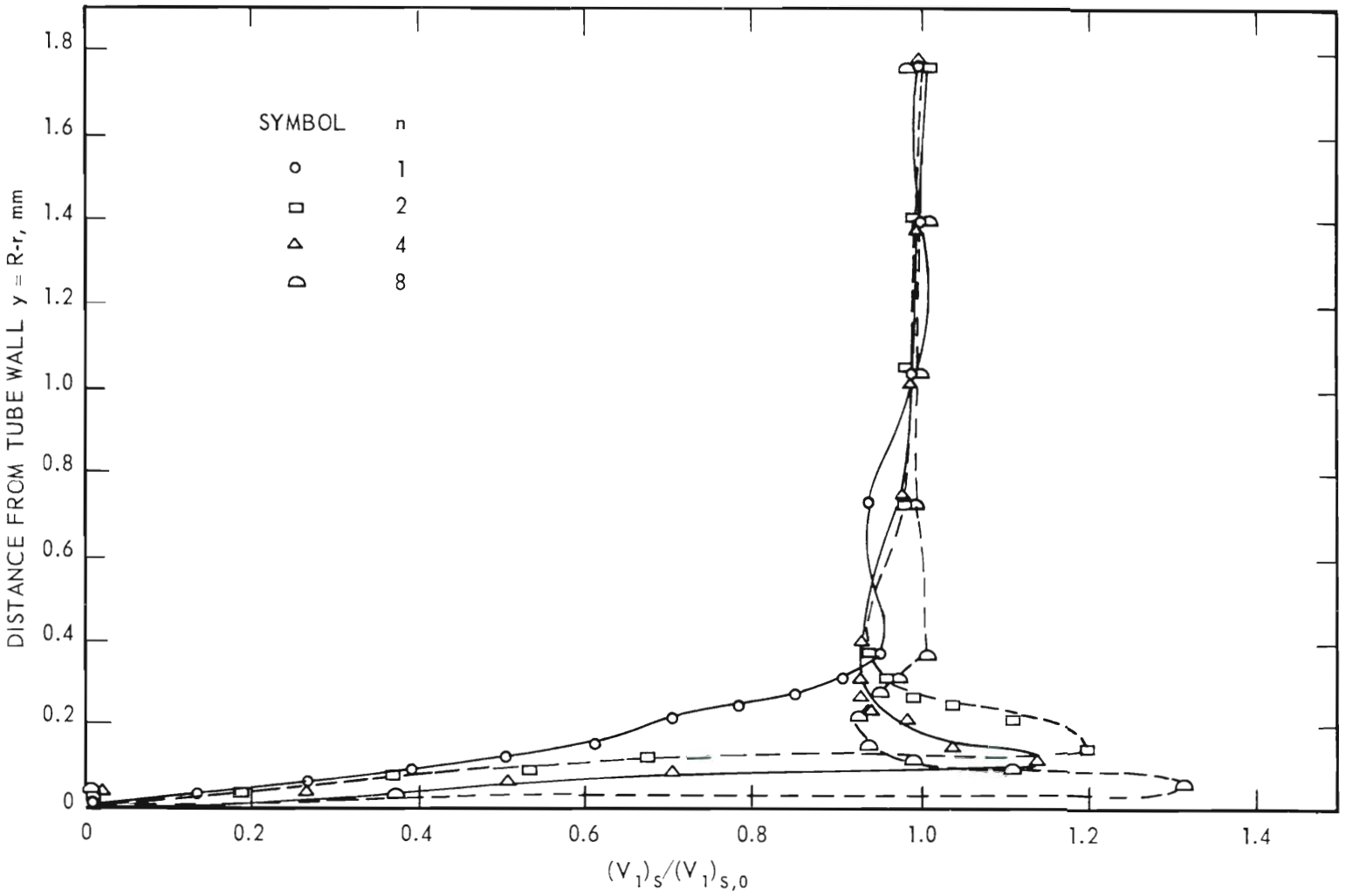

Figure 15. Velocity Profile Without Throughflow at a Point in the Domain of the Special Case as a Function of Sound Field Frequency; R = 0.116 ft.

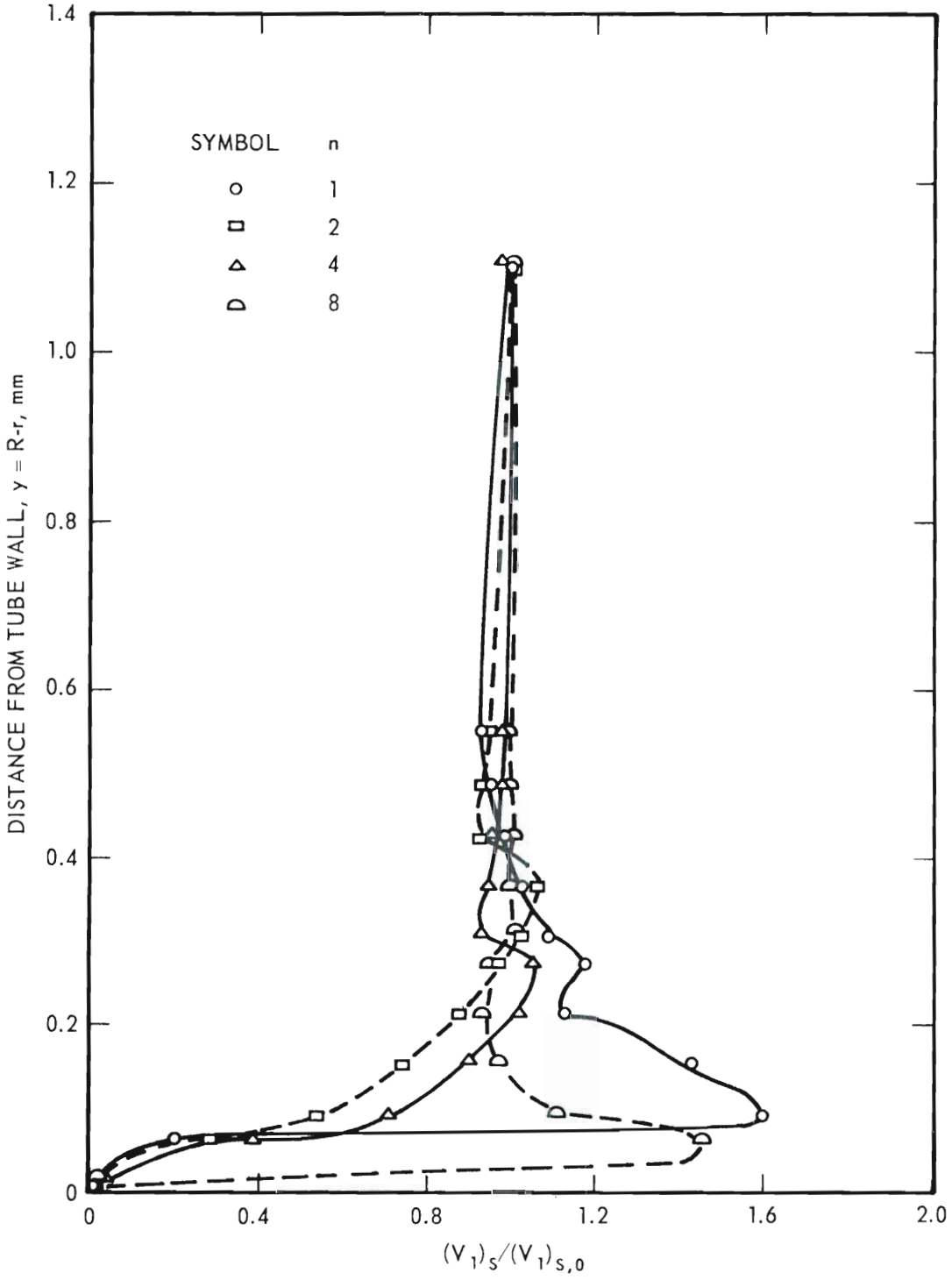

Figure 16. Velocity Profile Without Throughflow at a Point in the Domain of the Special Case as a Function of Sound Field Frequency; R = 0.174 ft.

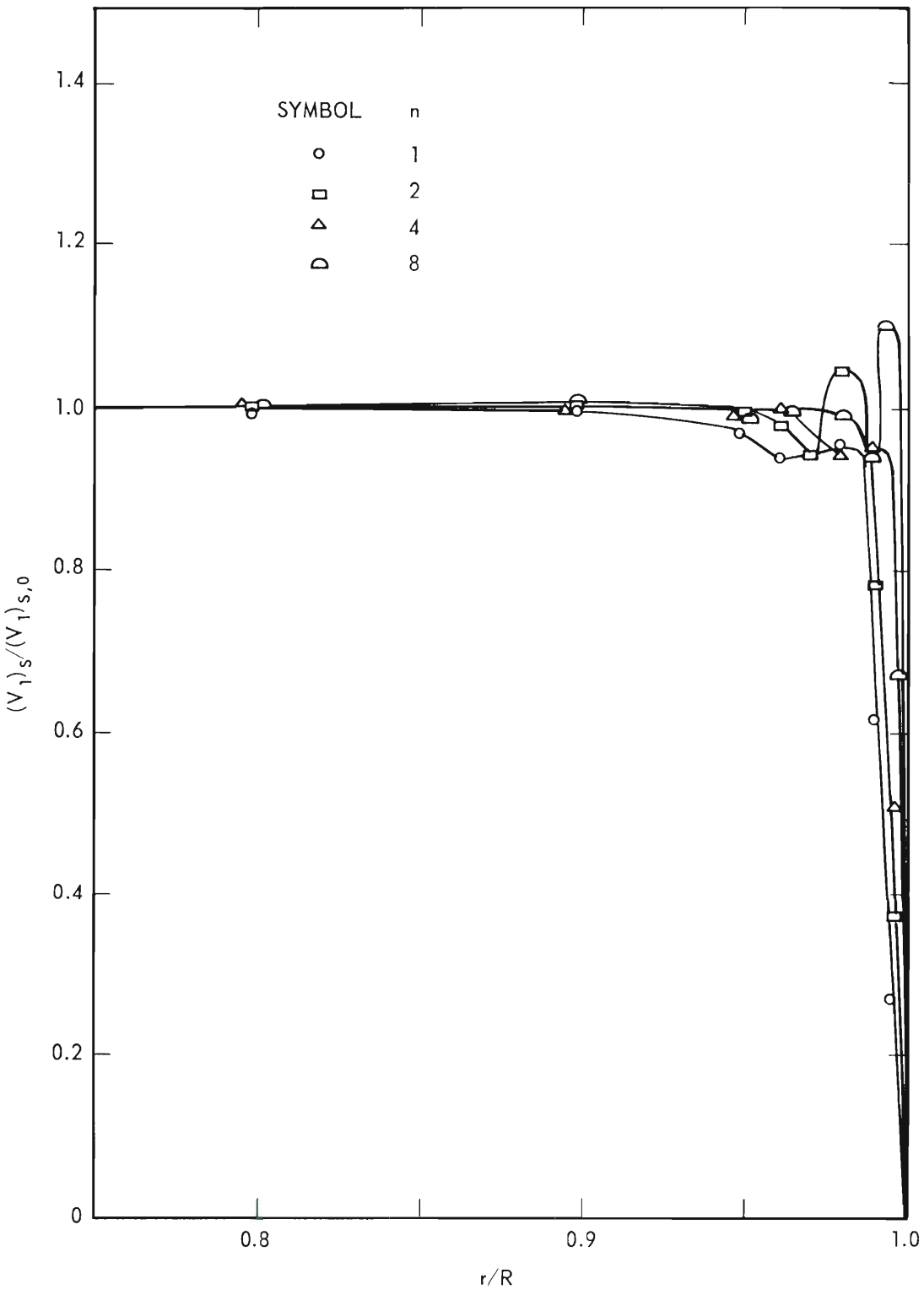

Figure 17. Velocity Distribution as a Function of Acoustic Frequency in the Domain of the Special Case and Without Throughflow; R = 0.058 ft.

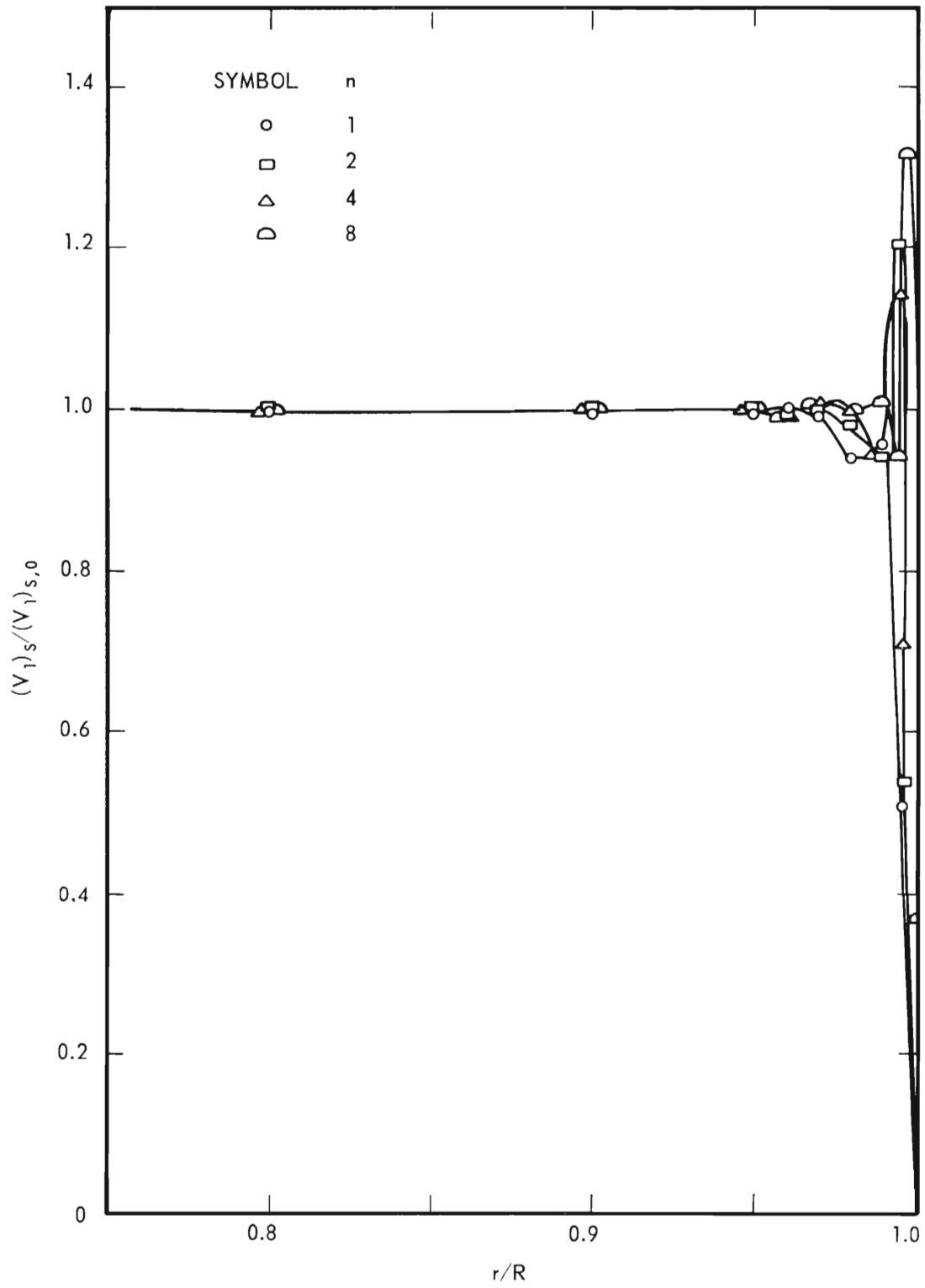

Figure 18. Velocity Distribution as a Function of Acoustic Frequency in the Domain of the Special Case and Without Throughflow; R = 0.116 ft.

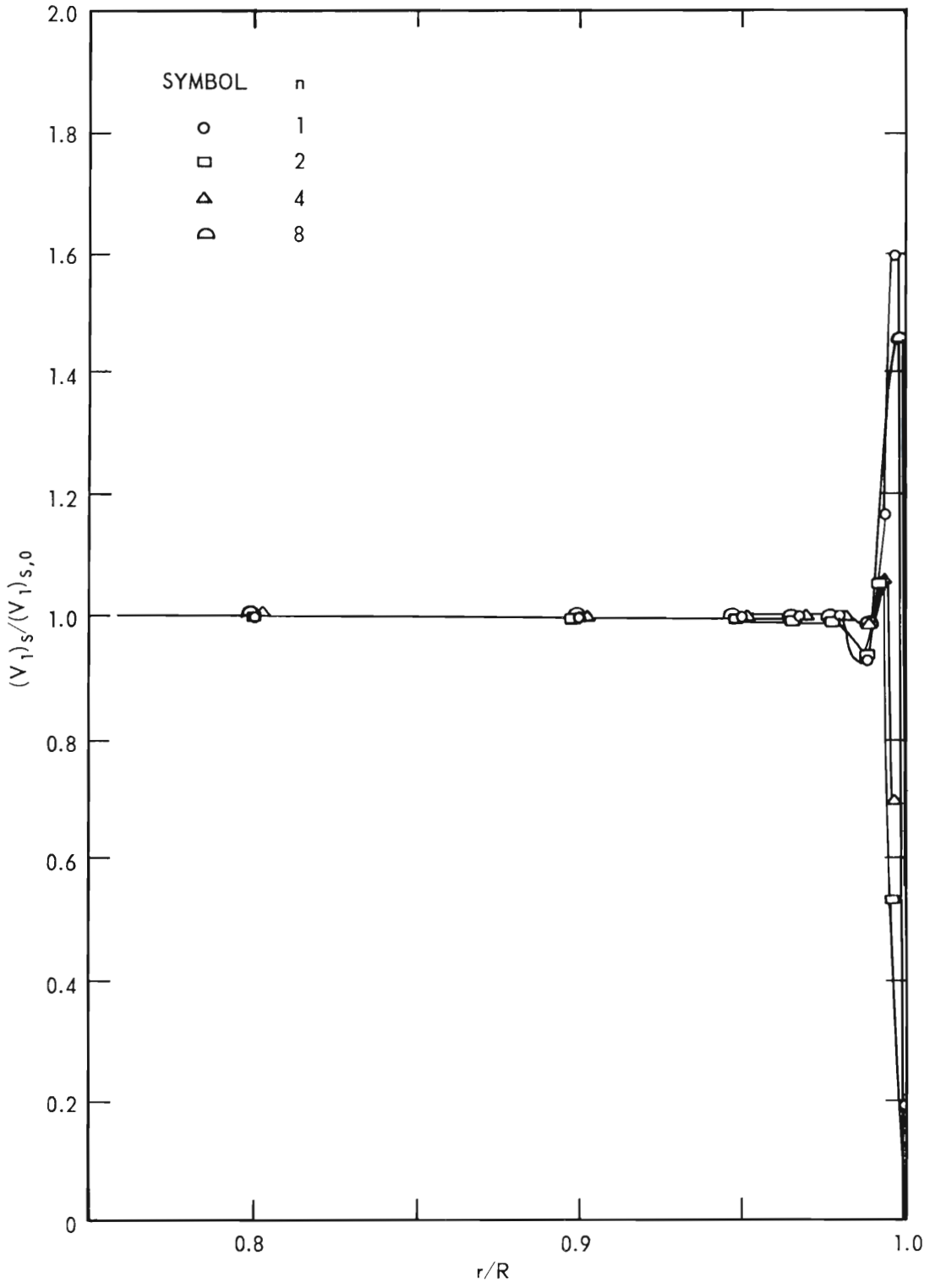

Figure 19. Velocity Distribution as a Function of Acoustic Frequency in the Domain of the Special Case and Without Throughflow; R = 0.174 ft.

of the tube consists of three major regions. The first of these regions includes the principal central portion of the tube in which $(V_1)_s$ is essentially uniform. The second region is the narrow portion of the tube within approximately 0.6mm from the tube wall in which complex changes in $(V_1)_s$ take place. The third region is the tube wall at which $(V_1)_s$ becomes zero. Consideration of the first and third regions alone permits the determination of simplified expressions for $(U_1)_s$ for the principal portion of the tube cross-section.

The continuity equation for the general analytical system can be written in a form similar to Equation (1), or

$$\frac{\partial U}{\partial r} + \frac{U}{r} + \frac{\partial V}{\partial z} = 0 \ . \tag{63}$$

The combination of Equations (2), (3) and (63) yields

$$\frac{\partial U_o}{\partial r} + \frac{U_o}{r} + \frac{\partial V_o}{\partial z} = - e^{i\omega t}\left(\frac{\partial U_1}{\partial r} + \frac{U_1}{r} + \frac{\partial V_1}{\partial r}\right) \ . \tag{64}$$

The left side of this equation is identical with the continuity equation for steady flow which can be expressed in the form

$$\frac{\partial U_o}{\partial r} + \frac{U_o}{r} + \frac{\partial V_o}{\partial z} = 0. \tag{65}$$

When Equation (65) is substituted into Equation (64), the result is an expression for the continuity equation in terms of U_1 and V_1 in the form

$$\frac{\partial U_1}{\partial r} + \frac{U_1}{r} = - \frac{\partial V_1}{\partial z} \ . \tag{66}$$

In the bulk of the tube cross-section identified as the first region, the expression for $(V_1)_s$ given in Equation (60) is applicable. From Equation (60)

$$\frac{\partial (V_1)_{s,b}}{\partial z} = \frac{n\nu\pi^2 P_r \, e^{SPL/8.68}}{L^2 \mu \omega_f} \sin (n\pi z/L) , \tag{67}$$

where the subscript b refers to the bulk of the tube cross-section. The substitution of Equation (67) into Equation (66) yields

$$\frac{\partial (U_1)_{s,b}}{\partial r} + \frac{(U_1)_{s,b}}{r} = - \frac{n\nu\pi^2 P_r \, e^{SPL/8.68}}{L^2 \mu \omega_f} \sin (n\pi z/L) . \tag{68}$$

Equation (68) has the general solution

$$(U_1)_{s,b} = - \frac{rn\nu\pi^2 P_r \, e^{SPL/8.68}}{2L^2 \mu \omega_f} \sin (n\pi z/L) + C_3/r . \tag{69}$$

The imposition of the boundary condition that $(U_1)_{s,b}$ must be finite at the tube centerline requires that $C_3 = 0$. The final expression for $(U_1)_{s,b}$ becomes

$$(U_1)_{s,b} = - \frac{rn\nu\pi^2 P_r \, e^{SPL/8.68}}{2L^2 \mu \omega_f} \sin (n\pi z/L) . \tag{70}$$

The results of the calculation procedure for the determination of $(U_1)_{s,b}$ from Equation (70) are given in Tables 9 through 12. The ranges of the selected values for the various parameters used in this calculation procedure are the same as those selected for the evaluation

Table 9. Calculated Values of $(U_l)_s$ in a Tube with a Radius of 0.058 ft; n = 1

$n\pi z/L$	r/R	$(U_l)_s$, ft/sec				
	SPL:	140 db	145 db	150 db	155 db	160 db
0	All	0.0000	0.0000	0.0000	0.0000	0.0000
$\pi/4$	0.0	0.0000	0.0000	0.0000	0.0000	0.0000
	0.2	-0.0004	-0.0006	-0.0011	-0.0018	-0.0033
	0.4	-0.0006	-0.0011	-0.0021	-0.0037	-0.0066
	0.6	-0.0010	-0.0018	-0.0031	-0.0055	-0.0098
	0.8	-0.0013	-0.0023	-0.0042	-0.0074	-0.0132
	1.0	0.0000	0.0000	0.0000	0.0000	0.0000
$\pi/2$	0.0	0.0000	0.0000	0.0000	0.0000	0.0000
	0.2	-0.0005	-0.0008	-0.0015	-0.0026	-0.0047
	0.4	-0.0009	-0.0016	-0.0029	-0.0052	-0.0093
	0.6	-0.0014	-0.0025	-0.0044	-0.0078	-0.0139
	0.8	-0.0019	-0.0033	-0.0059	-0.0105	-0.0187
	1.0	0.0000	0.0000	0.0000	0.0000	0.0000
$3\pi/4$	0.0	0.0000	0.0000	0.0000	0.0000	0.0000
	0.2	-0.0004	-0.0006	-0.0011	-0.0018	-0.0033
	0.4	-0.0006	-0.0011	-0.0021	-0.0037	-0.0066
	0.6	-0.0010	-0.0018	-0.0031	-0.0055	-0.0098
	0.8	-0.0013	-0.0023	-0.0042	-0.0074	-0.0132
	1.0	0.0000	0.0000	0.0000	0.0000	0.0000
π	All	0.0000	0.0000	0.0000	0.0000	0.0000

Table 10. Calculated Values of $(U_l)_s$ in a Tube with a Radius of 0.058 ft; n = 8

$n\pi z/L$	r/R	$(U_l)_s$, ft/sec				
	SPL:	140 db	145 db	150 db	155 db	160 db
0	All	0.0000	0.0000	0.0000	0.0000	0.0000
$\pi/4$	0.0	0.0000	0.0000	0.0000	0.0000	0.0000
	0.2	-0.0032	-0.0048	-0.0088	-0.0144	-0.0264
	0.4	-0.0048	-0.0088	-0.0168	-0.0296	-0.0527
	0.6	-0.0080	-0.0144	-0.0248	-0.0440	-0.0783
	0.8	-0.0104	-0.0184	-0.0336	-0.0592	-0.1056
	1.0	0.0000	0.0000	0.0000	0.0000	0.0000
$\pi/2$	0.0	0.0000	0.0000	0.0000	0.0000	0.0000
	0.2	-0.0040	-0.0064	-0.0120	-0.0208	-0.0376
	0.4	-0.0072	-0.0128	-0.0232	-0.0416	-0.0744
	0.6	-0.0112	-0.0200	-0.0352	-0.0624	-0.1112
	0.8	-0.0152	-0.0264	-0.0472	-0.0840	-0.1496
	1.0	0.0000	0.0000	0.0000	0.0000	0.0000
$3\pi/4$	0.0	0.0000	0.0000	0.0000	0.0000	0.0000
	0.2	-0.0032	-0.0048	-0.0088	-0.0144	-0.0264
	0.4	-0.0048	-0.0088	-0.0168	-0.0296	-0.0527
	0.6	-0.0080	-0.0144	-0.0248	-0.0440	-0.0783
	0.8	-0.0104	-0.0184	-0.0336	-0.0592	-0.1056
	1.0	0.0000	0.0000	0.0000	0.0000	0.0000
π	All	0.0000	0.0000	0.0000	0.0000	0.0000

(Continued)

Table 10 (Continued). Calculated Values of $(U_l)_s$ in a Tube with a Radius of 0.058 ft; $n = 8$

$n\pi z/L$	r/R	$(U_l)_s$, ft/sec				
	SPL:	140 db	145 db	150 db	155 db	160 db
$5\pi/4$	0.0	0.0000	0.0000	0.0000	0.0000	0.0000
	0.2	0.0032	0.0048	0.0088	0.0144	0.0264
	0.4	0.0048	0.0088	0.0168	0.0296	0.0527
	0.6	0.0080	0.0144	0.0248	0.0440	0.0783
	0.8	0.0104	0.0184	0.0336	0.0592	0.1056
	1.0	0.0000	0.0000	0.0000	0.0000	0.0000
$3\pi/2$	0.0	0.0000	0.0000	0.0000	0.0000	0.0000
	0.2	0.0040	0.0064	0.0120	0.0208	0.0376
	0.4	0.0072	0.0128	0.0232	0.0416	0.0744
	0.6	0.0112	0.0200	0.0352	0.0624	0.1112
	0.8	0.0152	0.0264	0.0472	0.0840	0.1496
	1.0	0.0000	0.0000	0.0000	0.0000	0.0000
$7\pi/4$	0.0	0.0000	0.0000	0.0000	0.0000	0.0000
	0.2	0.0032	0.0048	0.0088	0.0144	0.0264
	0.4	0.0048	0.0088	0.0168	0.0296	0.0527
	0.6	0.0080	0.0144	0.0248	0.0440	0.0783
	0.8	0.0104	0.0184	0.0336	0.0592	0.1056
	1.0	0.0000	0.0000	0.0000	0.0000	0.0000
2π	All	0.0000	0.0000	0.0000	0.0000	0.0000

Table 11. Calculated Values of $(U_1)_s$ in a Tube with a Radius of 0.174 ft; $n^1=^s 1$

$n\pi z/L$	r/R	$(U_1)_s$, ft/sec				
		SPL: 140 db	145 db	150 db	155 db	160 db
0	All	0.0000	0.0000	0.0000	0.0000	0.0000
$\pi/4$	0.0	0.0000	0.0000	0.0000	0.0000	0.0000
	0.2	-0.0012	-0.0018	-0.0033	-0.0054	-0.0099
	0.4	-0.0018	-0.0033	-0.0063	-0.0111	-0.0198
	0.6	-0.0030	-0.0054	-0.0093	-0.0165	-0.0294
	0.8	-0.0039	-0.0069	-0.0126	-0.0222	-0.0396
	1.0	0.0000	0.0000	0.0000	0.0000	0.0000
$\pi/2$	0.0	0.0000	0.0000	0.0000	0.0000	0.0000
	0.2	-0.0015	-0.0024	-0.0045	-0.0078	-0.0141
	0.4	-0.0027	-0.0048	-0.0087	-0.0156	-0.0279
	0.6	-0.0042	-0.0075	-0.0132	-0.0234	-0.0417
	0.8	-0.0057	-0.0099	-0.0177	-0.0315	-0.0561
	1.0	0.0000	0.0000	0.0000	0.0000	0.0000
$3\pi/4$	0.0	0.0000	0.0000	0.0000	0.0000	0.0000
	0.2	-0.0012	-0.0018	-0.0033	-0.0054	-0.0099
	0.4	-0.0018	-0.0033	-0.0063	-0.0111	-0.0198
	0.6	-0.0030	-0.0054	-0.0093	-0.0165	-0.0294
	0.8	-0.0039	-0.0069	-0.0126	-0.0222	-0.0396
	1.0	0.0000	0.0000	0.0000	0.0000	0.0000
π	All	0.0000	0.0000	0.0000	0.0000	0.0000

Table 12. Calculated Values of $(U_l)_s$ in a Tube with a Radius of 0.174 ft; $n^1=^s 8$

$n\pi z/L$	r/R	$(U_l)_s$, ft/sec				
		SPL: 140 db	145 db	150 db	155 db	160 db
0	All	0.0000	0.0000	0.0000	0.0000	0.0000
$\pi/4$	0.0	0.0000	0.0000	0.0000	0.0000	0.0000
	0.2	-0.0096	-0.0144	-0.0264	-0.0432	-0.0792
	0.4	-0.0144	-0.0264	-0.0504	-0.0888	-0.1581
	0.6	-0.0240	-0.0432	-0.0744	-0.1320	-0.2349
	0.8	-0.0312	-0.0552	-0.1008	-0.1776	-0.3168
	1.0	0.0000	0.0000	0.0000	0.0000	0.0000
$\pi/2$	0.0	0.0000	0.0000	0.0000	0.0000	0.0000
	0.2	-0.0120	-0.0192	-0.0360	-0.0624	-0.1128
	0.4	-0.0216	-0.0384	-0.0696	-0.1248	-0.2232
	0.6	-0.0336	-0.0600	-0.1056	-0.1872	-0.3336
	0.8	-0.0456	-0.0792	-0.1416	-0.2520	-0.4488
	1.0	0.0000	0.0000	0.0000	0.0000	0.0000
$3\pi/4$	0.0	0.0000	0.0000	0.0000	0.0000	0.0000
	0.2	-0.0096	-0.0144	-0.0264	-0.0432	-0.0792
	0.4	-0.0144	-0.0264	-0.0504	-0.0888	-0.1581
	0.6	-0.0240	-0.0432	-0.0744	-0.1320	-0.2349
	0.8	-0.0312	-0.0552	-0.1008	-0.1776	-0.3168
	1.0	0.0000	0.0000	0.0000	0.0000	0.0000
π	All	0.0000	0.0000	0.0000	0.0000	0.0000

(Continued)

Table 12 (Continued). Calculated Values of $(U_1)_s$ in a Tube with a Radius of 0.174 ft; $n^1=^s 8$

$n\pi z/L$	r/R	$(U_1)_s$, ft/sec				
	SPL:	140 db	145 db	150 db	155 db	160 db
$5\pi/4$	0.0	0.0000	0.0000	0.0000	0.0000	0.0000
	0.2	0.0096	0.0144	0.0264	0.0432	0.0792
	0.4	0.0144	0.0264	0.0504	0.0888	0.1581
	0.6	0.0240	0.0432	0.0744	0.1320	0.2349
	0.8	0.0312	0.0552	0.1008	0.1776	0.3168
	1.0	0.0000	0.0000	0.0000	0.0000	0.0000
$3\pi/2$	0.0	0.0000	0.0000	0.0000	0.0000	0.0000
	0.2	0.0120	0.0192	0.0360	0.0624	0.1128
	0.4	0.0216	0.0384	0.0696	0.1248	0.2232
	0.6	0.0336	0.0600	0.1056	0.1872	0.3336
	0.8	0.0456	0.0792	0.1416	0.2520	0.4488
	1.0	0.0000	0.0000	0.0000	0.0000	0.0000
$7\pi/4$	0.0	0.0000	0.0000	0.0000	0.0000	0.0000
	0.2	0.0096	0.0144	0.0264	0.0432	0.0792
	0.4	0.0144	0.0264	0.0504	0.0888	0.1581
	0.6	0.0240	0.0432	0.0744	0.1320	0.2349
	0.8	0.0312	0.0552	0.1008	0.1776	0.3168
	1.0	0.0000	0.0000	0.0000	0.0000	0.0000
2π	All	0.0000	0.0000	0.0000	0.0000	0.0000

of $(V_1)_s$, the results of which were given in Tables 2 through 5 and Figs. 10 through 13.

In the third region of the tube cross-section at the tube wall, the applicable expression for $(V_1)_s$ is Equation (51). When differentiated with respect to z, Equation (51) yields the result

$$\frac{\partial (V_1)_s}{\partial z} = - \frac{n\nu\pi^2 P_r \, e^{SPL/8.68}}{L^2 \mu \omega_f} \left[\frac{M_o[r(n\omega_f/\nu)^{1/2}]}{M_o[R(n\omega_f/\nu)^{1/2}]} \cos \left\{ (\Theta_o)_r - (\Theta_o)_R \right\} - 1 \right] \sin (n\pi z/L) \, .$$

This last expression becomes zero at the tube wall since both $M_o[r(n\omega_f/\nu)^{1/2}]/M_o[R(n\omega_f/\nu)^{1/2}]$ and $\cos \left\{ (\Theta_o)_r - (\Theta_o)_R \right\}$ reduce to unity. As a result, Equation (66) becomes

$$\frac{d(U_{1,R})}{dr} + \frac{(U_{1,R})}{r} = 0 \, . \tag{71}$$

Equation (71) has the general solution

$$(U_{1,R}) = C_4/r \, . \tag{72}$$

The boundary condition $U_1 = 0$ at $r = R$ requires that C_4 be identically zero such that Equation (72) reduces to

$$(U_{1,R}) = 0$$

which is required of the expression for U_1.

Determination of the values of V_o at any point (r,z).--The results of Langhaar's analytical study provide a rapid method for the evaluation of the steady-flow velocity component in the z-direction for a tube under conditions of laminar-flow development. This method requires the specification of the throughflow Reynolds number Re, the tube radius R, the axial position in the tube z, the radial position in the tube r, and the kinematic viscosity of the fluid ν. The prescribed values for Re, R and z are combined to give a value for the expression 2z/RRe. From this value and the results of Langhaar's work given in Fig. 24 in the Appendix a corresponding value for βR is obtained. From this value of βR and the prescribed values for R and r, an evaluation of the Bessel functions I_o (βR), I_2 (βR) and I_o (βr) can be obtained from tables such as those compiled by Jahnke and Emde (18). The combination of these values for the Bessel functions yields an expression for V_o in the form

$$V_o/V_{mo} = [I_o (\beta R) - I_o (\beta r)]/I_2 (\beta R)$$

where

$$V_{mo} = Re\nu/2R \ .$$

Since V_{mo} can be evaluated from the prescribed values for Re, R and ν, the desired value for V_o at a point (r,z) can also be obtained. Tables 13 through 15 give the results of the numerical evaluation of V_o for a tube four feet long through which air is flowing under conditions of laminar flow development. Reynolds numbers of 100, 1000 and 2000, and tube radii of 0.058 ft, 0.116 ft and 0.174 ft were used to obtain the results given in these tables.

Table 13. Values of V_o Calculated by the Method of Langhaar; Re = 100

Axial Position	Radial Position	V_o, ft/sec		
z/L	r/R	R: 0.058 ft	0.116 ft	0.174 ft
0.0000	0.0	0.26	0.13	0.09
	0.2	0.26	0.13	0.09
	0.4	0.26	0.13	0.09
	0.6	0.26	0.13	0.09
	0.8	0.26	0.13	0.09
0.0625	0.0	0.48	0.21	0.14
	0.2	0.47	0.21	0.14
	0.4	0.42	0.20	0.13
	0.6	0.34	0.17	0.12
	0.8	0.21	0.11	0.08
	1.0	0.00	0.00	0.00
0.1250	0.0	0.52	0.24	0.15
	0.2	0.50	0.23	0.15
	0.4	0.44	0.21	0.14
	0.6	0.33	0.17	0.11
	0.8	0.19	0.10	0.07
	1.0	0.00	0.00	0.00
0.2500	0.0	0.52	0.26	0.17
	0.2	0.49	0.25	0.16
	0.4	0.44	0.22	0.15
	0.6	0.33	0.16	0.12
	0.8	0.18	0.09	0.07
	1.0	0.00	0.00	0.00
0.3750	0.0	0.52	0.26	0.18
	0.2	0.49	0.25	0.17
	0.4	0.44	0.22	0.15
	0.6	0.33	0.16	0.11
	0.8	0.18	0.09	0.06
	1.0	0.00	0.00	0.00

(Continued)

Table 13 (Continued). Values of V_o Calculated by the Method of Langhaar; Re = 100

Axial Position	Radial Position	V_o, ft/sec		
z/L	r/R	R: 0.058 ft	0.116 ft	0.174 ft
0.5000	0.0	0.52	0.26	0.18
	0.2	0.49	0.25	0.17
	0.4	0.44	0.22	0.15
	0.6	0.33	0.16	0.11
	0.8	0.18	0.09	0.06
	1.0	0.00	0.00	0.00
0.6250	0.0	0.52	0.26	0.18
	0.2	0.49	0.25	0.17
	0.4	0.44	0.22	0.15
	0.6	0.33	0.16	0.11
	0.8	0.18	0.09	0.06
	1.0	0.00	0.00	0.00
0.7500	0.0	0.52	0.26	0.18
	0.2	0.49	0.25	0.17
	0.4	0.44	0.22	0.15
	0.6	0.33	0.16	0.11
	0.8	0.18	0.09	0.06
	1.0	0.00	0.00	0.00
0.8750	0.0	0.52	0.26	0.18
	0.2	0.49	0.25	0.17
	0.4	0.44	0.22	0.15
	0.6	0.33	0.16	0.11
	0.8	0.18	0.09	0.06
	1.0	0.00	0.00	0.00
1.0000	0.0	0.52	0.26	0.18
	0.2	0.49	0.25	0.17
	0.4	0.44	0.22	0.15
	0.6	0.33	0.16	0.11
	0.8	0.18	0.09	0.06
	1.0	0.00	0.00	0.00

Table 14. Values of V_o Calculated by the Method of Langhaar; Re = 1000

Axial Position	Radial Position	V_o, ft/sec		
z/L	r/R	R: 0.058 ft	0.116 ft	0.174 ft
0.0000	0.0	2.59	1.29	0.86
	0.2	2.59	1.29	0.86
	0.4	2.59	1.29	0.86
	0.6	2.59	1.29	0.86
	0.8	2.59	1.29	0.86
0.1250	0.0	3.75	1.72	1.10
	0.2	3.73	1.72	1.10
	0.4	3.63	1.69	1.09
	0.6	3.29	1.61	1.06
	0.8	2.41	1.27	0.88
	1.0	0.00	0.00	0.00
0.2500	0.0	4.25	1.87	1.19
	0.2	4.17	1.86	1.18
	0.4	3.91	1.81	1.16
	0.6	3.36	1.64	1.08
	0.8	2.25	1.20	0.83
	1.0	0.00	0.00	0.00
0.3750	0.0	4.43	2.03	1.25
	0.2	4.32	2.00	1.24
	0.4	4.02	1.91	1.20
	0.6	3.34	1.68	1.09
	0.8	2.12	1.16	0.80
	1.0	0.00	0.00	0.00
0.5000	0.0	4.58	2.12	1.31
	0.2	4.45	2.08	1.29
	0.4	4.07	1.95	1.18
	0.6	3.31	1.68	1.10
	0.8	2.07	1.12	0.77
	1.0	0.00	0.00	0.00

(Continued)

Table 14 (Continued). Values of V_o Calculated by the Method of Langhaar; Re = 1000

Axial Position	Radial Position	V_o, ft/sec		
z/L	r/R	R: 0.058 ft	0.116 ft	0.174 ft
0.6250	0.0	4.83	2.16	1.35
	0.2	4.66	2.12	1.33
	0.4	4.19	1.96	1.26
	0.6	3.39	1.66	1.10
	0.8	2.05	1.08	0.75
	1.0	0.00	0.00	0.00
0.7500	0.0	4.87	2.21	1.41
	0.2	4.72	2.16	1.38
	0.4	4.19	2.00	1.30
	0.6	3.31	1.66	1.12
	0.8	1.94	1.06	0.75
	1.0	0.00	0.00	0.00
0.8750	0.0	4.97	2.23	1.44
	0.2	4.79	2.17	1.41
	0.4	4.24	2.00	1.32
	0.6	3.31	1.64	1.13
	0.8	1.99	1.01	0.75
	1.0	0.00	0.00	0.00
1.0000	0.0	5.00	2.28	1.44
	0.2	4.82	2.22	1.41
	0.4	4.24	2.03	1.31
	0.6	3.31	1.65	1.10
	0.8	1.94	1.03	0.71
	1.0	0.00	0.00	0.00

Table 15. Values of V_o Calculated by the Method of Langhaar; Re = 2000

Axial Position	Radial Position	V_o, ft/sec		
z/L	r/R	R: 0.058 ft	0.116 ft	0.174 ft
0.0000	0.0	5.17	2.59	1.72
	0.2	5.17	2.59	1.72
	0.4	5.17	2.59	1.72
	0.6	5.17	2.59	1.72
	0.8	5.17	2.59	1.72
0.3750	0.0	8.12	3.60	2.29
	0.2	8.01	3.60	2.29
	0.4	7.65	3.50	2.25
	0.6	6.72	3.27	2.15
	0.8	4.65	2.48	1.70
	1.0	0.00	0.00	0.00
0.5000	0.0	8.47	3.75	2.37
	0.2	8.32	3.73	2.36
	0.4	7.80	3.62	2.32
	0.6	6.72	3.29	2.17
	0.8	4.49	2.41	1.67
	1.0	0.00	0.00	0.00
0.6250	0.0	8.63	3.93	2.43
	0.2	8.47	3.88	2.41
	0.4	7.85	3.73	2.36
	0.6	6.67	3.34	2.17
	0.8	4.34	2.38	1.62
	1.0	0.00	0.00	0.00

(Continued)

Table 15 (Continued). Values of V_o Calculated by the Method of Langhaar; Re = 2000

Axial Position	Radial Position	V_o, ft/sec		
z/L	r/R	R: 0.058 ft	0.116 ft	0.174 ft
0.7500	0.0	8.83	4.07	2.49
	0.2	8.62	4.02	2.48
	0.4	8.01	3.83	2.41
	0.6	6.67	3.37	2.19
	0.8	4.23	2.33	1.60
	1.0	0.00	0.00	0.00
0.8750	0.0	8.94	4.09	2.58
	0.2	8.68	4.02	2.56
	0.4	8.01	3.81	2.48
	0.6	6.56	3.31	2.24
	0.8	4.03	2.23	1.62
	1.0	0.00	0.00	0.00
1.0000	0.0	9.15	4.25	2.62
	0.2	8.89	4.17	2.58
	0.4	8.11	3.91	2.36
	0.6	6.61	3.37	2.20
	0.8	4.13	2.25	1.55
	1.0	0.00	0.00	0.00

CHAPTER VI

DISCUSSION OF RESULTS

Domain of applicability of the special case.--The results given in Table 1 and Fig. 9 describe the scope of the domain in the analytical system in which the effects of β are negligible in the solution for the general case. It can be seen from Fig. 9 that within the laminar-flow regime for a tube with a length of four feet and with a radius greater than 5×10^{-2} ft (0.60 in), β is negligible beyond an inlet length of 3.60 inches. This length decreases with an increase in tube radius or a decrease in the throughflow Reynolds number due to the rapidity with which the laminar boundary layer develops in pipes at lower values of Reynolds number.

These important results lead to the conclusion that β may be neglected in the analytical model for the principal length of the tube. This results in the applicability of the simplified solution for the velocity profile due to acoustic vibrations provided by Equation (51). The evaluation of this equation involves a calculation procedure much less time-consuming than that required for the evaluation of the solution for the general case in which β cannot be neglected.

The fact that β becomes negligible in the expression for V_1 has practical significance in that V_1 becomes independent of V_o and all throughflow effects in the domain where β is negligible. This establishes the applicability of Equation (51) in the determination of the velocity

profile in a resonant tube in the absence of throughflow. Under these conditions, the domain of the special case includes the entire system except for a very small region at the tube inlet. As a result of this fact, the solution for the general case was not evaluated in this study.

Velocity effects due to sound in the absence of throughflow.--The fact that the acoustically-resonant closed tube has received much greater analytical and experimental treatment than has the open tube was discussed in Chapter I. The open-tube and closed-tube systems differ in their analysis under conditions of resonance due principally to the difference in the values of z/L at which velocity loops and nodes exist. The physical location of these loops and nodes in the open tube was described in Chapter III. In the closed tube, both ends of the tube are velocity nodes, and velocity loops are spaced at a distance of $\lambda/4$ between successive nodes. Under conditions when the acoustic fields in the tubes are produced by progressive waves instead of by standing waves as in the case of resonance, the analytical treatments for the closed-tube and open-tube systems should be similar.

The resonance restriction was imposed upon the procedure for the derivation of Equation (51) by the conditions included in Equation (9). This restriction resulted in the periodic variation of $(V_1)_{s,0}$ with z shown in Figs. 10 through 13. The amplitudes or absolute values of these velocity variations can be obtained by replacing the term cos $(n\pi z/L)$ by unity in Equation (60). When this absolute value for $(V_1)_{s,0}$ is included in Equation (61), the resonance restriction becomes removed from the velocity profiles given in Figs. 14 through 19. This permits a comparison between the analytical results given in these

figures and the experimental and analytical results reported by Meyer and Güth (4) for a closed tube in which progressive waves of similar frequencies were established. A comparison is given in Fig. 20 between the analytical results calculated from Equation (61) at a frequency of 137 cycles per second for tube radii of 0.058 ft and 0.116 ft with results reported by Meyer and Güth for 60 and 100 cycles per second. The agreement between the experimental and the analytical values for the thickness of the boundary layer due to acoustic vibrations is excellent. This agreement indicates that the restrictions employed in the development of the analytical model can also be applied to the model for the practical system without the introduction of serious errors. Experimental data for higher frequencies were not available for a comparison with the other analytical results given in Figs. 14 through 19.

The values for $(V_1)_s$ provided by Figs. 10 through 19 and the values for $(U_1)_s$ given in Tables 9 through 12 can be combined to yield an interpretation of the instantaneous velocity effects which take place in the system in the absence of throughflow. The instantaneous direction and magnitude of the resultant velocity vector at any point (r,z) in the system are determined by the direction and magnitude of the corresponding axial and radial velocity components $(V_1)_s$ and $(U_1)_s$, respectively, at that instant. A qualitative analysis of the effects of $(V_1)_s$ and $(U_1)_s$ on the resultant velocity vector can be obtained from a consideration of the general characteristics of the velocity components indicated by Figs. 10 through 19 and Tables 9 through 12.

The general behaviour of $(V_1)_s$ is a periodic variation with respect to axial position with maximum effects taking place at values of

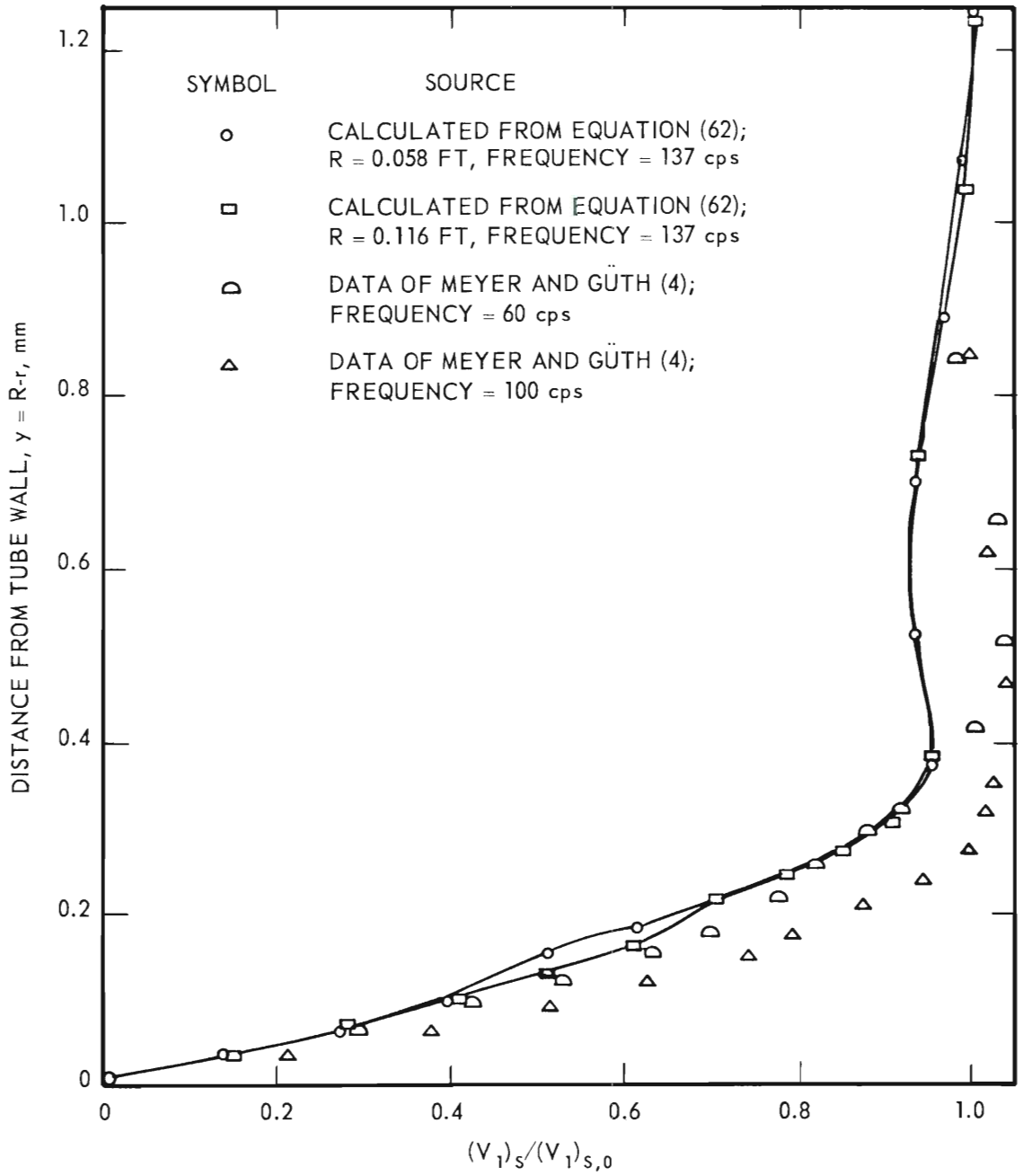

Figure 20. Comparison Between Analytical and Experimental Velocity Profiles Due to Acoustic Vibrations.

cos ($n\pi z/L$) equal to positive and negative unity, but with no effects at values of cos ($n\pi z/L$) equal to zero. The variation of $(V_1)_s$ with respect to radial position is essentially negligible except in a region very near the tube wall. Increases in the frequency of the acoustic disturbance increase the number of nodes and loops and decrease the spacing between successive nodes and loops; however, the magnitude of $(V_1)_s$ is not changed by these increases in n except in the region near the tube wall. Increases in the sound pressure level of the acoustic field produce large increases in the magnitude of $(V_1)_s$.

The variation of $(U_1)_s$ is periodic with respect to axial position with maximum effects taking place at values of sin ($n\pi z/L$) equal to psoitive and negative unity, but with no effects at values of sin ($n\pi z/L$) equal to zero. Therefore, $(U_1)_s$ is 90 degrees out of phase with $(V_1)_s$ such that maximum effects due to $(U_1)_s$ take place where $(V_1)_s = 0$. The magnitude of $(U_1)_s$ also varies with respect to radial position. At the tube centerline and at the tube wall, $(U_1)_s$ is zero, but between these points $(U_1)_s$ increases with increasing r until the narrow region near the tube wall is encountered. Tables 9 through 12 further indicate that $(U_1)_s$ increases greatly with increases in acoustic frequency and sound pressure level. The maximum values given for $(U_1)_s$ in these tables are not as great as the maximum values obtained for $(V_1)_s$ under the same conditions of frequency and sound pressure level.

The combination of these general effects indicates that for a tube with a given length and radius an increase in sound pressure level increases both the axial and radial velocity components. An increase in the frequency of the acoustic disturbance increases the number of

locations along the length of the tube at which maximum and minimum effects due to $(V_1)_s$ and $(U_1)_s$ are produced. These increases in frequency do not increase the magnitude of $(V_1)_{s,0}$ but they do increase $(U_1)_s$. In a similar manner, for the range of values of tube radii included in the evaluations in Chapter V, increases in R produced increases in $(U_1)_s$ but did not affect $(V_1)_{s,0}$. These general effects indicate that the influence of $(U_1)_s$ on the resultant velocity vector at a point increases with an increase in frequency and tube radius. A schematic representation of the instantaneous trends in the direction and magnitude of the radial and axial velocity components and the resultant velocity vector at a point in the tube is shown in Fig. 21.

A review of the results of Jackson and Johnson (3) which were discussed in Chapter I provides an interesting comparison with these general trends predicted by the analytical model. These investigators obtained flow patterns with smoke over a wide range of resonant frequencies in closed tubes of various diameters. The geometrical arrangement of these circulatory flow patterns was observed to be greatly dependent upon the tube radius and the frequency of the resonant field. In tubes having small diameters the flow cells were axially directed and symmetrical with respect to the tube axis at lower frequencies. At higher frequencies the cells shifted to a radial orientation with less axial symmetry. In tubes of larger diameter only the cells with the radial orientation could be produced. Photographs of these effects are shown in Figs. 3 and 4.

Combined velocity effects due to sound and throughflow.--The combination of the values calculated for $(V_1)_s$ and V_o results in an evaluation

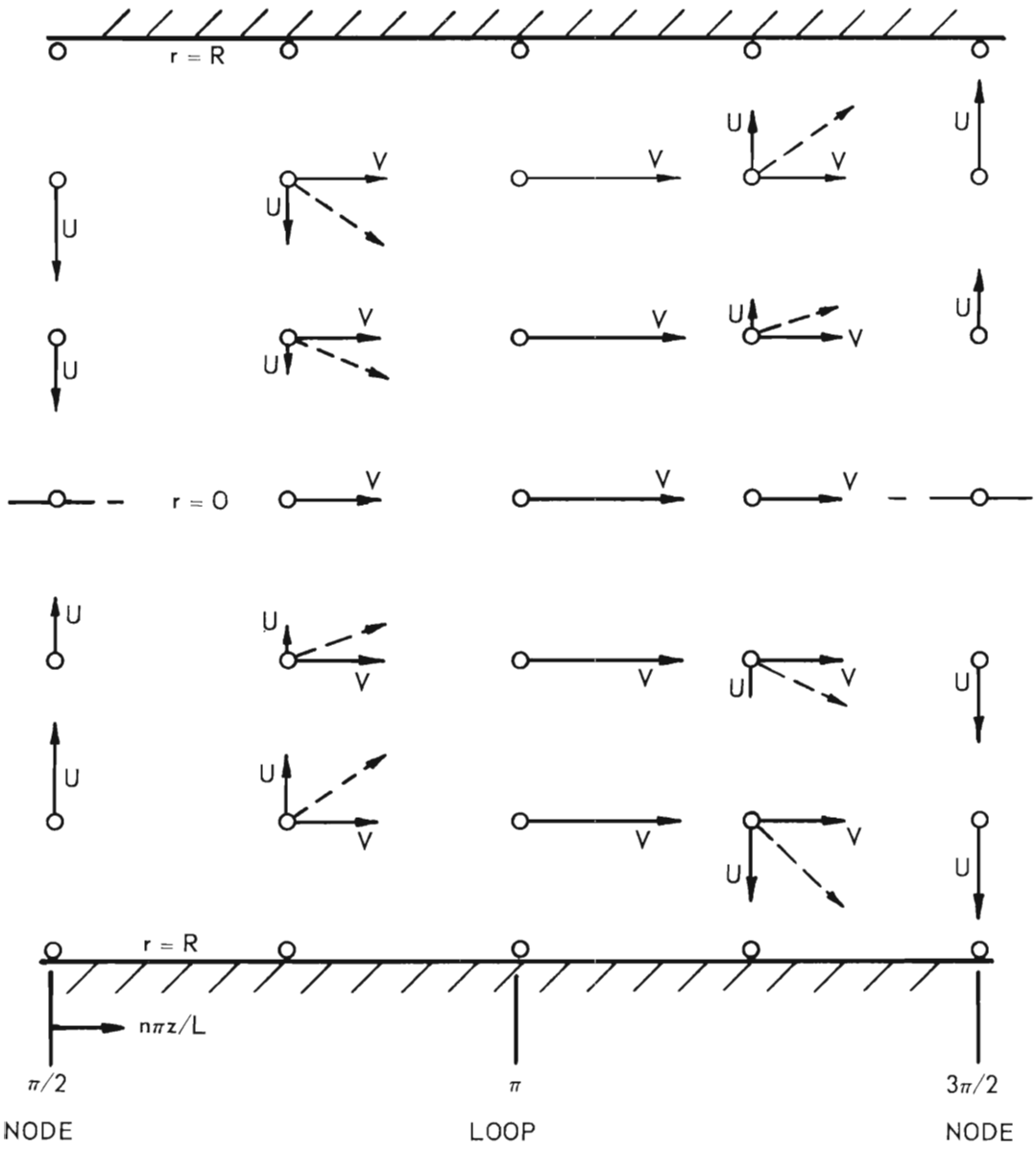

Figure 21. Schematic Representation of the Instantaneous Velocity Vectors Due to Acoustic Vibrations in a System Without Throughflow.

of the total instantaneous velocity component in the axial direction. The results of typical combinations of these values are shown in Figs. 22 and 23. In both of these figures the radius of the tube is 0.116 ft, the frequency is the first harmonic resonant frequency for a tube four feet long, and the sound pressure level is 160 decibels. In Fig. 22, a low Reynolds number of 100 is designated. At this Reynolds number the laminar boundary layer would normally develop rapidly to yield a parabolic velocity profile in the absence of a resonant acoustic field. In the case depicted, however, the value of $(V_1)_s$ is large with respect to V_o at velocity loops and is the controlling factor in the determination of the resultant axial velocity vector at these points. At the velocity nodes, $(V_1)_s$ is zero and the velocity profile is the same as that produced at these axial positions in the absence of acoustical effects. The periodic variation of the velocity effects due to acoustic vibrations with respect to time and axial position produces the various changes in the magnitude and direction of the velocity profiles shown in Fig. 22.

In Fig. 23, a higher Reynolds number of 1000 is prescribed. At this Reynolds number the normal boundary-layer development is slower but the values of V_o at a point are larger. The values of $(V_1)_s$ are not large enough to cause the reversals in flow direction shown in Fig. 22; however, they are large enough to affect the shape of the velocity profiles. As in the case shown in Fig. 22, no effects are produced on the normal velocity profiles at the velocity nodes; however, effects which are periodic with respect to axial position and time are produced at all other axial locations.

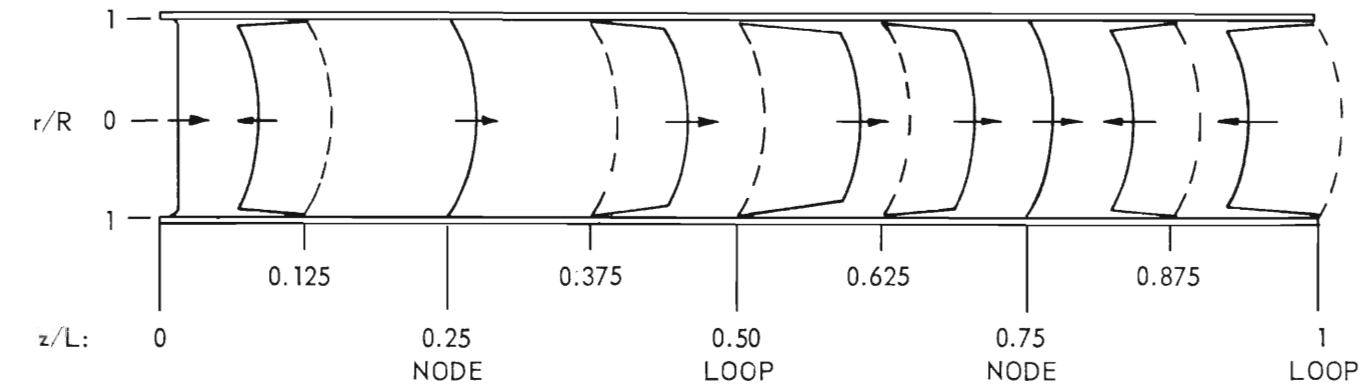

a. AT TIME t

NORMAL PROFILE

PROFILE INFLUENCED BY ACOUSTIC VIBRATIONS

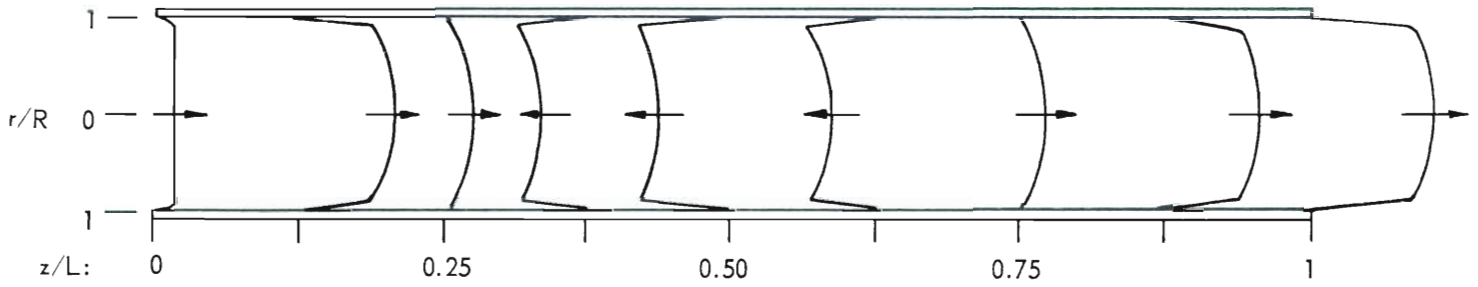

b. AT TIME ONE-HALF PERIOD LATER THAN t

Figure 22. Representation of Instantaneous Velocity Profiles Due to the Effects of Resonant Acoustic Vibrations and Throughflow in a Tube; R = 0.116 ft, Re = 100, n = 2, and SPL = 160 db.

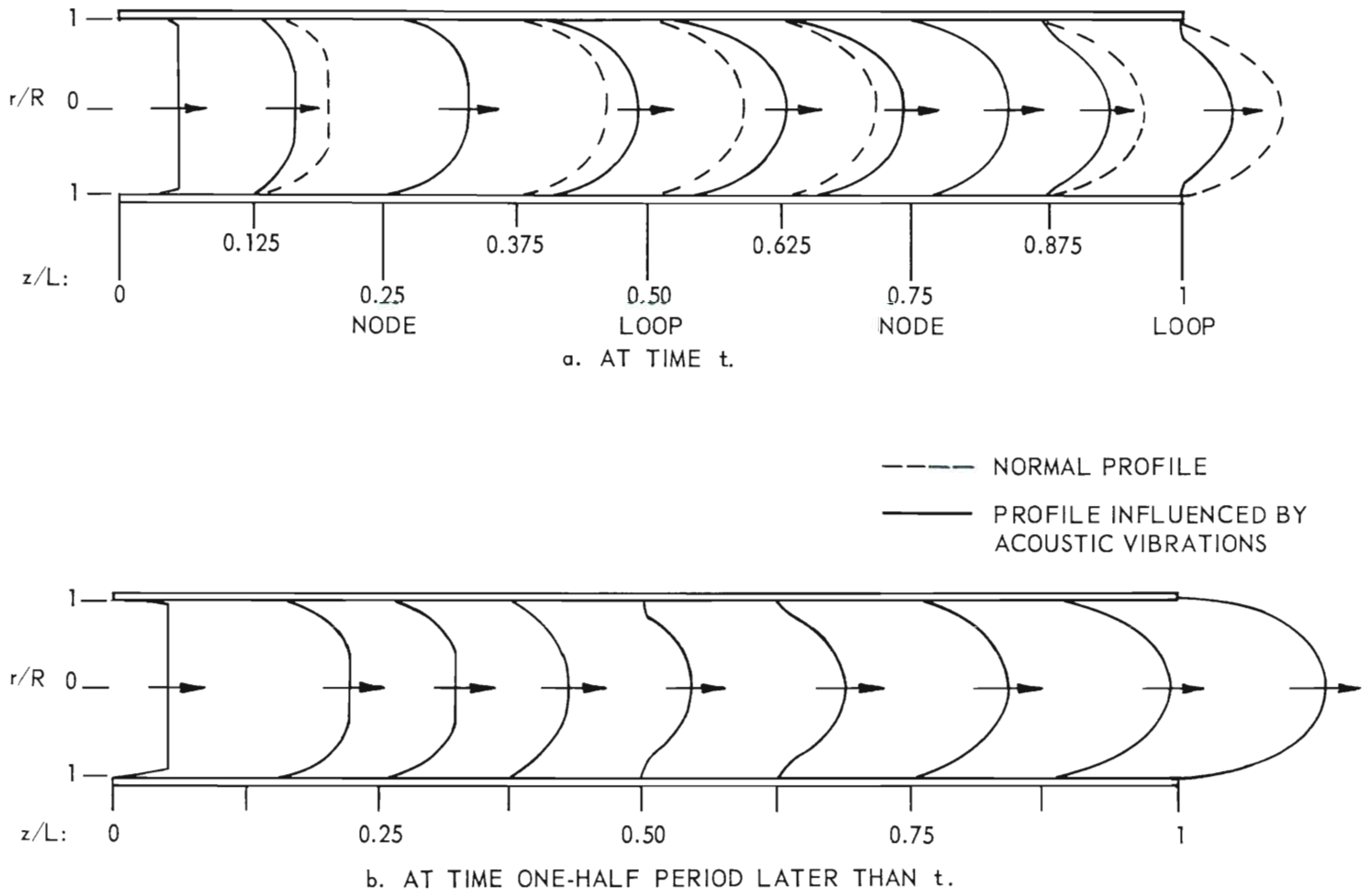

Figure 23. Representation of Instantaneous Velocity Profiles Due to the Effects of Resonant Acoustic Vibrations and Throughflow in a Tube; R = 0.116 ft, Re = 1000, n = 2, and SPL = 160 db.

The general trends indicated by combinations of this type provide a qualitative basis for comparison with results of experimental investigations. One of the trends indicated in Figs. 22 and 23 is the periodic increase and decrease in the thickness of the normal boundary layer which would develop in the absence of acoustical effects. The greatest changes in the normal boundary-layer thickness occur at velocity loops. At velocity nodes, no changes are produced. A second trend is the effect of frequency on the resultant velocity profiles. A change of frequency would not affect the magnitude of $(V_1)_s$ but would alter the locations at which minimum and maximum combined effects are produced. Finally, any decrease in the sound pressure level would produce a decrease in the magnitude of $(V_1)_s$. This predicts that below a particular "threshold" sound pressure level the effects of $(V_1)_s$ on the velocity profiles in the tube would be insignificant. This "threshold" sound pressure level would necessarily depend upon the values of V_o which are dependent upon the value of the throughflow Reynolds number for the system. All of these trends predicted by the analytical model for the system with throughflow have been observed experimentally by Jackson, Harrison and Boteler (10), Spurlock, et al. (11), and Jackson, et al. (12).

CHAPTER VII

CONCLUSIONS AND RECOMMENDATIONS

An analytical model for the effects of resonant acoustic vibrations on air in an open horizontal tube has been presented. Solutions to this model were derived for cases with and without throughflow effects. The solution which includes the effects of throughflow was based upon the assumption that laminar-flow development prevails in the analytical system. The following conclusions resulted from this study:

1. The resonant acoustical effects on the air velocity in the analytical system are not dependent upon the throughflow effects over the entire tube length except for a small region at the tube inlet.

2. The absolute values of the velocity profiles calculated from the solution of the analytical model for the case without throughflow effects give good agreement with experimental data obtained for progressive sound waves of approximately the same frequency in the region of a solid boundary.

3. The instantaneous directions and magnitudes of the resultant of the radial and axial velocity components due to acoustical effects in the analytical system are greatly influenced by the values of the tube radius and the frequency of the acoustic disturbance. Over the range of values included in this investigation, increases in either or both of these parameters resulted in a greater influence on the resultant vector by the radial velocity component.

4. The solution to the analytical model for the system with throughflow predicts an instantaneous acoustic effect on the normal laminar boundary-layer development which is periodic with respect to axial position in the system. There are no effects at the tube inlet and at velocity nodes, whereas maximum effects occur at velocity loops other than the tube inlet.

It is recommended that further investigations involving experimental as well as additional analytical studies be conducted. The following studies are suggested:

1. Additional analytical development should be undertaken to yield an expression for the mean velocity effects due to acoustic vibrations over an entire vibration period. An expression of this type could then be incorporated into the appropriate rate equation to yield expressions for the effects of resonant acoustic vibrations on transport rates.

2. Additional flow visualization studies should be conducted to provide more experimental observations of the effects of acoustic vibrations on boundary-layer development. The previous investigations which studied the velocity profiles due to acoustic vibrations in the region of a solid surface should be continued to provide data for higher frequencies and sound pressure levels.

APPENDIX

SUMMARY OF LANGHAAR'S RESULTS

Langhaar (13) obtained an expression for the determination of velocity profiles due to laminar-flow development in the entrance length of tubes. This expression was employed in the evaluation of the steady-flow velocity component in the axial direction, V_o, in Chapter V. In addition, the development employed by Langhaar in the derivation of this expression for V_o provided the basis for the technique employed in Chapter II to linearize the z-component of the Navier-Stokes equations of motion. A summary of the development used by Langhaar and the results of this development provide a better understanding of the method by which V_o was evaluated in Chapter V.

Langhaar employed the approximation

$$U_o(\partial V_o/\partial r) + V_o(\partial V_o/\partial z) = \nu\beta^2 V_o$$

to reduce the z-component of the Navier-Stokes equations of motion in cylindrical coordinates for steady flow to the form

$$\frac{\partial^2 V_o}{\partial r^2} + \frac{1}{r}\frac{\partial V_o}{\partial r} - \beta^2 V_o = \frac{1}{\mu}\left(\frac{\partial P_o}{\partial z}\right) . \tag{73}$$

Equation (73) applies to a system in which the density and viscosity of the fluid in the system are constant, the effects of gravity are negligible and axial symmetry exists. It was assumed that $\partial^2 V_o/\partial z^2$ is negligible in the z-component of the equations of motion. Finally, the

expression $\partial P_o/\partial z$ was considered to be a function of z alone. These restrictions yield a general solution to Equation (73) which consists of the solution to the complementary equation

$$\frac{\partial^2 V_o}{\partial r^2} + \frac{1}{r}\frac{\partial V_o}{\partial r} - \beta^2 V_o = 0 \tag{74}$$

and the particular solution

$$V_o = -\alpha_o/\beta^2 , \tag{75}$$

where

$$\alpha_o = \frac{1}{\mu}\frac{\partial P_o}{\partial z} .$$

Equation (74) has the form of the modified Bessel equation of the first kind of zero order. The only solution to Equation (74) which is finite when r = 0, as required by the physical system is

$$V_o = C_1 I_o(\beta r) .$$

The general solution to Equation (73) then becomes

$$V_o = C_1 I_o(\beta r) - (\alpha_o/\beta^2) . \tag{76}$$

The substitution of the boundary condition that $V_o = 0$ when r = R into Equation (76) yields

$$C_1 I_o(\beta R) = \alpha_o/\beta^2 . \tag{77}$$

The continuity equation for steady flow can be written in the form

$$\int_0^R rV_o \, dr = R^2 V_{mo}/2 \ , \tag{78}$$

where

$$V_{mo} = Re\nu/2R \ .$$

The combination of Equations (76) and (78) yields the expression

$$\int_0^R r\left[C_1 I_o(\beta r) - (\alpha_o/\beta^2)\right] dr = R^2 V_{mo}/2$$

which becomes

$$\frac{RC_1 I_1(\beta R)}{\beta} - \frac{\alpha_o R^2}{2\beta^2} = \frac{R^2 V_{mo}}{2} \ . \tag{79}$$

The simultaneous solution of Equations (77) and (79) yields expressions for the constants C_1 and α_o in the forms

$$C_1 = RV_{mo}/\left[\frac{2I_1(\beta R)}{\beta} - RI_o(\beta R)\right] \tag{80}$$

and

$$\alpha_o = R\beta^2 V_{mo} I_o(\beta R)/\left[\frac{2I_1(\beta R)}{\beta} - RI_o(\beta R)\right] \ . \tag{81}$$

The combination of Equations (76), (80) and (81) gives the expression

$$V_o = \frac{RV_{mo}\left[I_o(\beta r) - I_o(\beta R)\right]}{\left[\frac{2I_1(\beta R)}{\beta} - RI_o(\beta R)\right]} \ ,$$

which reduces to

$$V_o = \frac{V_{mo}\ [I_o(\beta R) - I_o(\beta r)]}{I_2(\beta R)} \quad . \tag{82}$$

The remainder of Langhaar's development yielded an expression for β as a function of z. This expression was numerically evaluated to give the results shown in Fig. 24. These results can then be incorporated into Equation (82) to provide a method for the evaluation of the velocity profiles due to the steady-state development of laminar flow in the entrance length of a tube.

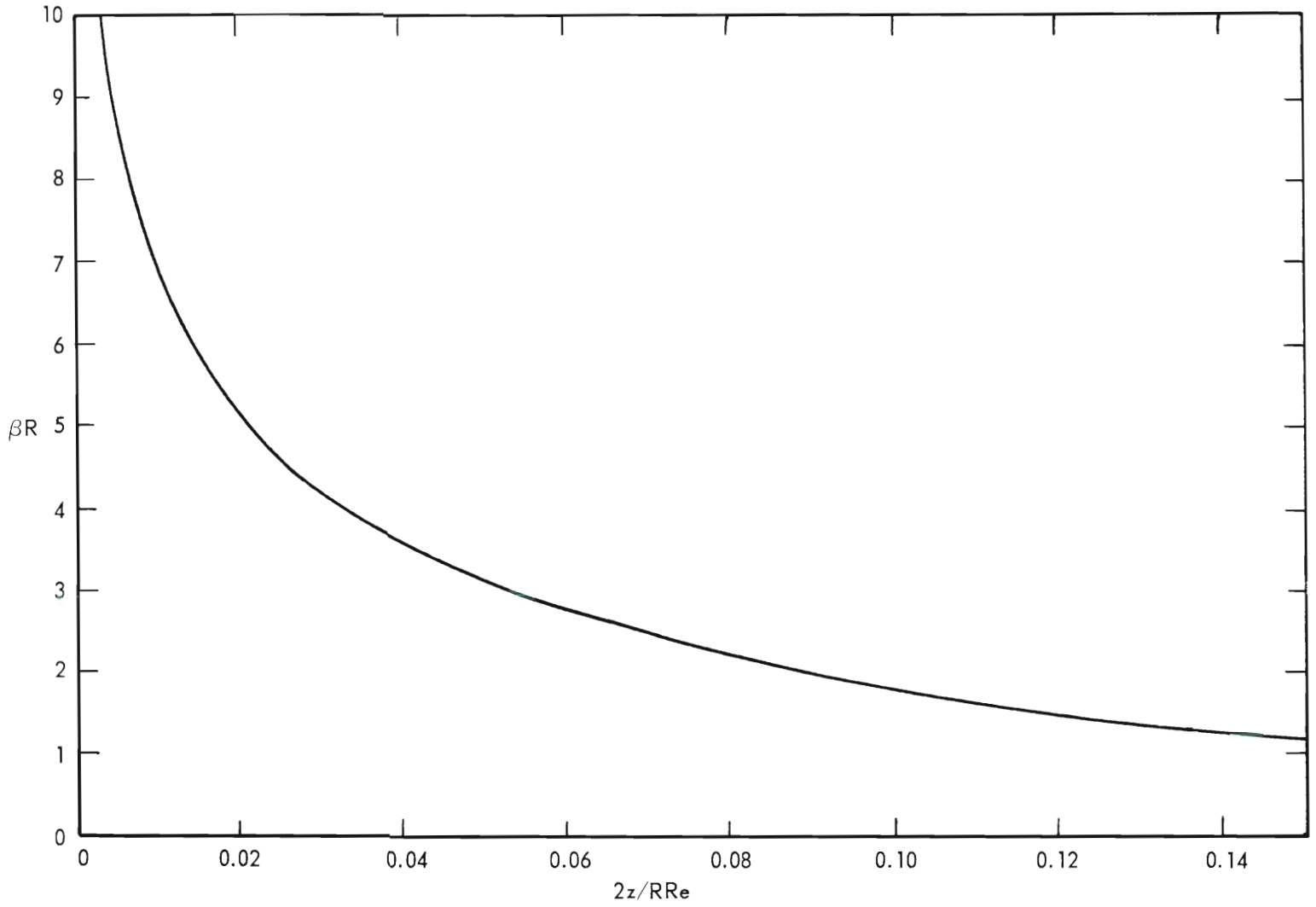

Figure 24. Representation of βR as a Function of 2z/RRe from the Results of Langhaar (13).

BIBLIOGRAPHY

1. Lord Rayleigh, "On the Circulation of Air Observed in Kundt's Tubes and on Some Allied Acoustical Problems", Philosophical Transactions of the Royal Society of London, 75, Part I (1884), pp. 1-21.

2. Andrade, E. N. da C., "On the Circulations Caused by the Vibrations of Air in a Tube", Proceedings of the Royal Society of London, Series A, 134, (1932), pp. 445-470.

3. Jackson, T. W., and H. L. Johnson, "Convective Flow Due to Acoustic Vibrations in Horizontal Resonant Tubes", AFOSR Technical Report 60-52, (1960).

4. Meyer, E., and W. Güth, "Zur Akustischen Zähigkeitsgrenzschicht", Acustica, 3, (1953), pp. 185-187.

5. Cremer, L., "Über der akustische Grenzschicht vor starren Wänden", Archiv der elektrischen Ubertragung, 2, (1948), pp. 136-139.

6. Holman, J. P. and T. P. Mott-Smith, "The Effect of High Constant Pressure Sound Fields on Free Convection Heat Transfer from a Horizontal Cylinder", WADC Technical Note 58-352, (ASTIA Document No. AD 206906), Wright Air Development Center, (1958).

7. Kubanskii, P. N., "Effect of Acoustical Vibrations of Finite Amplitude on the Boundary Layer", Zhurnal Technicheskoi Fiziki, 22, (1952), pp. 593-601.

8. Kubanskii, P. N., "Currents Around a Heated Solid in a Standing Acoustic Wave", Transactions of the Academy of Sciences (U. S. S. R.), LXXXII, No. 4, (1953), pp. 585-588.

9. Kubanskii, P. N., "Flow Near a Heated Hard Body in a Standing Acoustic Wave", Zhurnal Technicheskoi Fiziki, 22, (1952), pp. 585-592.

10. Jackson, T. W., W. B. Harrison, and W. C. Boteler, "Free Convection, Forced Convection, and Acoustic Vibrations in a Constant Temperature Vertical Tube", Transactions of the American Society of Mechanical Engineers, Series C, 81, (1959), pp. 68-74.

11. Spurlock, J. M., T. W. Jackson, K. R. Purdy, C. C. Oliver, and H. L. Johnson, "The Effects of Resonant Acoustic Vibrations on Heat Transfer to Air in Horizontal Tubes", WADC Technical Note 59-330, Wright Air Development Center, (1959).

12. Jackson, T. W., K. R. Purdy, C. C. Oliver and H. L. Johnson, "The Effects of Resonant Acoustic Vibrations on the Local and Overall Heat Transfer Coefficients for Air Flowing Through an Isothermal Horizontal Tube", ARL Technical Report 60-322, Aeronautical Research Laboratory, (1960).

13. Langhaar, H. L., "Steady Flow in the Transition Length of a Straight Tube", Journal of Applied Mechanics, 9, (1942), pp. 55-58.

14. Peterson, A. P. G., and L. L. Beranek, Handbook of Noise Measurement, General Radio Company, (1956).

15. National Bureau of Standards, Table of the Bessel Functions $J_o(z)$ and $J_1(z)$ for Complex Arguments, New York: Columbia University Press, (1943).

16. McLachlan, N. W., Bessel Functions for Engineers, Oxford: Oxford University Press, (1934).

17. Kreith, F., Principles of Heat Transfer, Scranton: International Textbook Company, (1958).

18. Jahnke, E., and F. Emde, Tables of Functions with Formulae and Curves, 4th ed., New York: Dover Publications, (1945).

VITA

Jack Marion Spurlock was born in Tampa, Florida, on August 16, 1930. He attended elementary schools in Tampa and Miami, Florida, and was graduated from Miami Edison High School. In 1948 he entered the University of Florida, from which he graduated in 1952, receiving the degree of Bachelor of Chemical Engineering. After graduation he entered the United States Air Force as a second lieutenant. He served two years as an armament test officer and was discharged at the end of his tour of duty with the rank of first lieutenant in the Air Force Reserve. In 1954 he was employed by the Auto-Lite Battery Company as a process and quality control engineer. He joined the staff of the Engineering Experiment Station of the Georgia Institute of Technology in 1955 as an assistant research engineer and enrolled in the Graduate Division of the Georgia Institute of Technology in 1956. He was awarded the degree of Master of Science in Chemical Engineering in 1958, after which he became an instructor in the School of Chemical Engineering and began his work towards the Ph.D. degree. Since this time he has been a member of the staff of the School of Chemical Engineering.

He now has the rank of captain in the Air Force Reserve and has been the instructor of the Research and Development Officers Training Flight of the Atlanta Air Reserve Center. He is a member of the American Chemical Society, the Society of Sigma Xi, the American Institute of Chemical Engineers, the Air Force Association and the American Society for Engineering Education.

In 1952 he was married to the former Phyllis Lowene Ridgway of Miami, Florida. They have a daughter, Barbara Lynn, and two sons, Scott Edward and Paul Andrew.